Supplementary Materials for

Gentrification drives patterns of alpha and beta diversity in cities

Mason Fidino *et al.*

Corresponding author: Mason Fidino, mfidino@lpzoo.org

The PDF file includes:

Methods

Biological sampling

We used data from 23 UWIN cities in the United States (U.S.) for this study. Each city followed the same systematic study design, placing motion-triggered camera traps in urban greenspace along an urbanization gradient (see Magle et al. 2019 for details). Mammal data for this study came from 12 distinct sampling periods between 2019 and 2021. Camera deployments in each sampling period were about 35 days (sd = 13.01) and began on the first of January, April, July, or October of each year. Because UWIN cities joined the network at different times, the number of sampling periods among cities varied (median = 7, minimum = 2, maximum = 12). The median number of unique camera-trapping sites per city was 35 (minimum = 23, maximum = 104).

Mammals in camera trap images were identified to species by trained experts. However, flying squirrel, gray squirrel, and cottontail rabbit species were summarized to either the subgenus or genus level given challenges in identifying them to the species level from camera trap images (Kays et al. 2022). For each camera deployment we counted the number of days each species was detected and the number of operational camera days, which were then used to estimate species occupancy and detectability within our multi-city multi-species occupancy model (Sutherland et al. 2016, Magle et al. 2021).

Overall, 48 mammal species were photographed but our multi-city, multi-species occupancy model converged when limited to the 21 species that were most frequently detected (a minimum of 75 detection days across at least 3 cities). Gray squirrels (Sciurus carolinensis or Sciurus griseus) were detected most often (~41,300 detection days) while flying squirrels (Glaucomys sp.) were detected the least (79 detection days). See Table S1 for a summary of species detected across cities.

Table S1: The number of sites species were detected and number of detections per city. This table included all species, not only those we could use in our analysis. Table is ordered by city, and within each city species are sorted from fewest to most detections.

	City	Species	Sites detected	Days detected
9	Athens, GA	striped skunk	3	9
2	Athens, GA	bobcat	7	31
8	Athens, GA	red fox	10	64
5	Athens, GA	gray fox	19	131
1	Athens, GA	armadillo	19	156
10	Athens, GA	virginia opossum	20	172
3	Athens, GA	cottontail sp	14	175
4	Athens, GA	coyote	17	191
7	Athens, GA	raccoon	24	335
6	Athens, GA	gray squirrel sp	27	839
11	Athens, GA	white tailed deer	27	1321
20	Bay Area, CA	north american river otter	1	1
19	Bay Area, CA	mule deer	1	6
22	Bay Area, CA	red fox	4	10
12	Bay Area, CA	bobcat	5	41
13	Bay Area, CA	california ground squirrel	3	45
16	Bay Area, CA	fox squirrel	8	132
14	Bay Area, CA	cottontail sp	10	180
17	Bay Area, CA	gray fox	6	208
24	Bay Area, CA	virginia opossum	9	271
23	Bay Area, CA	striped skunk	30	283
25	Bay Area, CA	white tailed deer	10	425
18	Bay Area, CA	gray squirrel sp	24	480

15	Bay Area, CA	coyote	39	954
21	Bay Area, CA	raccoon	41	1770
33	Boston, MA	north american mink	1	1
30	Boston, MA	flying squirrel sp	1	2
39	Boston, MA	weasel sp	1	2
41	Boston, MA	woodchuck	3	4
31	Boston, MA	gray fox	6	9
36	Boston, MA	red squirrel	4	13
37	Boston, MA	striped skunk	5	16
35	Boston, MA	red fox	8	23
38	Boston, MA	virginia opossum	11	41
29	Boston, MA	fisher	16	46
28	Boston, MA	eastern chipmunk	14	123
27	Boston, MA	coyote	21	243
40	Boston, MA	white tailed deer	22	361
26	Boston, MA	cottontail sp	23	385
34	Boston, MA	raccoon	26	436
32	Boston, MA	gray squirrel sp	27	1608
49	Chicago, IL	muskrat	1	1
47	Chicago, IL	gray fox	2	2
50	Chicago, IL	north american beaver	1	2
58	Chicago, IL	woodchuck	3	3
56	Chicago, IL	weasel sp	4	5
51	Chicago, IL	north american mink	10	16
45	Chicago, IL	flying squirrel sp	9	17
53	Chicago, IL	red fox	10	26
44	Chicago, IL	eastern chipmunk	28	194
54	Chicago, IL	striped skunk	46	365
43	Chicago, IL	coyote	78	914
46	Chicago, IL	fox squirrel	78	1159
55	Chicago, IL	virginia opossum	86	1554
42	Chicago, IL	cottontail sp	84	1814
57	Chicago, IL	white tailed deer	55	2563
52	Chicago, IL	raccoon	94	3062
48	Chicago, IL	gray squirrel sp	99	5516
59	Denver, CO	black bear	1	1
73	Denver, CO	virginia opossum	1	1
63	Denver, CO	cougar	2	2
68	Denver, CO	north american beaver	2	2
74	Denver, CO	white tailed deer	2	2
61	Denver, CO	bobcat	3	3
71	Denver, CO	red squirrel	2	3
65	Denver, CO	elk	3	10
72	Denver, CO	striped skunk	9	27
60	Denver, CO	black tailed prairie dog	9	29
62	Denver, CO	cottontail sp	18	107
64	Denver, CO	coyote	29	117
67	Denver, CO	mule deer	13	138
70	Denver, CO	red fox	24	147
69	Denver, CO	raccoon	27	252

66	Denver, CO	fox squirrel	37	1170
80	Houston, TX	gray fox	3	9
76	Houston, TX	bobcat	10	23
83	Houston, TX	striped skunk	4	31
85	Houston, TX	white tailed deer	2	49
78	Houston, TX	coyote	18	68
75	Houston, TX	armadillo	14	221
82	Houston, TX	raccoon	21	360
81	Houston, TX	gray squirrel sp	23	434
77	Houston, TX	cottontail sp	16	460
79	Houston, TX	fox squirrel	23	489
84	Houston, TX	virginia opossum	22	536
92	Indianapolis, IN	north american badger	1	1
98	Indianapolis, IN	striped skunk	2	3
91	Indianapolis, IN	muskrat	3	6
93	Indianapolis, IN	north american beaver	6	15
94	Indianapolis, IN	north american mink	9	37
88	Indianapolis, IN	eastern chipmunk	11	66
90	Indianapolis, IN	gray squirrel sp	21	155
97	Indianapolis, IN	red squirrel	19	181
96	Indianapolis, IN	red fox	31	220
101	Indianapolis, IN	woodchuck	16	240
87	Indianapolis, IN	coyote	37	422
100	Indianapolis, IN	white tailed deer	33	1091
99	Indianapolis, IN	virginia opossum	40	1743
86	Indianapolis, IN	cottontail sp	40	1798
89	Indianapolis, IN	fox squirrel	39	3786
95	Indianapolis, IN	raccoon	40	4658
106	Iowa City, IA	flying squirrel sp	1	1
110	Iowa City, IA	muskrat	1	1
112	Iowa City, IA	north american beaver	1	1
108	Iowa City, IA	gray fox	2	2
111	Iowa City, IA	north american badger	4	4
102	Iowa City, IA	bobcat	6	9
116	Iowa City, IA	striped skunk	12	34
113	Iowa City, IA	north american mink	19	61
119	Iowa City, IA	woodchuck	20	116
104	Iowa City, IA	coyote	34	309
105	Iowa City, IA	eastern chipmunk	19	311
115	Iowa City, IA	red fox	35	652
107	Iowa City, IA	fox squirrel	28	690
117	Iowa City, IA	virginia opossum	36	1202
103	Iowa City, IA	cottontail sp	35	1659
118	Iowa City, IA	white tailed deer	36	3281
109	Iowa City, IA	gray squirrel sp	37	3337
114	Iowa City, IA	raccoon	37	3878
129	Jackson, MS	striped skunk	3	8
121	Jackson, MS	bobcat	5	13
124	Jackson, MS	fox squirrel	4	13
123	Jackson, MS	coyote	14	46

125	Jackson, MS	gray fox	13	51
122	Jackson, MS	cottontail sp	12	82
120	Jackson, MS	armadillo	19	150
128	Jackson, MS	red fox	26	397
130	Jackson, MS	virginia opossum	34	641
131	Jackson, MS	white tailed deer	32	1054
127	Jackson, MS	raccoon	34	1162
126	Jackson, MS	gray squirrel sp	34	2469
141	Little Rock, AR	north american beaver	1	1
142	Little Rock, AR	north american mink	3	6
137	Little Rock, AR	flying squirrel sp	6	19
133	Little Rock, AR	bobcat	10	32
148	Little Rock, AR	woodchuck	8	36
136	Little Rock, AR	eastern chipmunk	5	55
144	Little Rock, AR	red fox	11	56
135	Little Rock, AR	coyote	23	89
145	Little Rock, AR	striped skunk	11	101
139	Little Rock, AR	gray fox	20	304
132	Little Rock, AR	armadillo	24	466
138	Little Rock, AR	fox squirrel	26	652
134	Little Rock, AR	cottontail sp	25	655
147	Little Rock, AR	white tailed deer	22	803
146	Little Rock, AR	virginia opossum	29	1647
143	Little Rock, AR	raccoon	28	1720
140	Little Rock, AR	gray squirrel sp	29	2285
154	Madison, WI	north american beaver	1	1
161	Madison, WI	woodchuck	1	1
155	Madison, WI	north american mink	1	3
152	Madison, WI	gray fox	1	4
159	Madison, WI	weasel sp	1	5
151	Madison, WI	eastern chipmunk	3	13
157	Madison, WI	striped skunk	4	16
150	Madison, WI	coyote	7	23
160	Madison, WI	white tailed deer	7	46
158	Madison, WI	virginia opossum	13	52
156	Madison, WI	raccoon	13	101
149	Madison, WI	cottontail sp	16	218
153	Madison, WI	gray squirrel sp	22	322
175	Metro LA, CA	white tailed deer	1	1
167	Metro LA, CA	eastern chipmunk	2	5
165	Metro LA, CA	cougar	3	8
169	Metro LA, CA	gray fox	8	76
168	Metro LA, CA	fox squirrel	16	79
172	Metro LA, CA	raccoon	23	114
170	Metro LA, CA	gray squirrel sp	7	127
173	Metro LA, CA	striped skunk	23	216
171	Metro LA, CA	mule deer	21	322
174	Metro LA, CA	virginia opossum	18	330
163	Metro LA, CA	california ground squirrel	20	386
162	Metro LA, CA	bobcat	26	394

166	Metro LA, CA	coyote	39	1535
164	Metro LA, CA	cottontail sp	28	1914
189	Phoenix, AZ	antelope ground squirrel	1	1
208	Phoenix, AZ	white tailed deer	1	1
202	Phoenix, AZ	north american beaver	1	3
192	Phoenix, AZ	cougar	8	20
203	Phoenix, AZ	north american river otter	6	25
196	Phoenix, AZ	hooded skunk	8	44
206	Phoenix, AZ	round tailed ground squirrel	10	53
201	Phoenix, AZ	north american badger	8	77
200	Phoenix, AZ	mule deer	16	154
207	Phoenix, AZ	striped skunk	17	181
199	Phoenix, AZ	kit fox	11	198
198	Phoenix, AZ	javelina	42	356
204	Phoenix, AZ	raccoon	46	429
190	Phoenix, AZ	bobcat	48	585
195	Phoenix, AZ	harris antelope squirrel	21	612
194	Phoenix, AZ	gray fox	40	655
205	Phoenix, AZ	rock squirrel	49	758
197	Phoenix, AZ	jackrabbit sp	46	2627
193	Phoenix, AZ	coyote	82	3855
191	Phoenix, AZ	cottontail sp	65	5190
216	Portland, Oregon	north american beaver	1	1
209	Portland, Oregon	california ground squirrel	1	3
219	Portland, Oregon	striped skunk	2	4
217	Portland, Oregon	north american river otter	1	7
221	Portland, Oregon	western chipmunk	2	15
212	Portland, Oregon	douglas squirrel	7	32
220	Portland, Oregon	virginia opossum	8	73
218	Portland, Oregon	raccoon	14	82
215	Portland, Oregon	mule deer	12	122
211	Portland, Oregon	coyote	19	159
210	Portland, Oregon	cottontail sp	18	183
213	Portland, Oregon	fox squirrel	19	238
214	Portland, Oregon	gray squirrel sp	19	370
229	Rochester, NY	north american beaver	1	1
230	Rochester, NY	north american mink	2	2
225	Rochester, NY	fisher	2	5
234	Rochester, NY	striped skunk	4	5
227	Rochester, NY	gray fox	5	11
226	Rochester, NY	flying squirrel sp	3	17
233	Rochester, NY	red squirrel	8	40
223	Rochester, NY	coyote	13	53
237	Rochester, NY	woodchuck	8	58
222	Rochester, NY	cottontail sp	12	108
235	Rochester, NY	virginia opossum	19	126
224	Rochester, NY	eastern chipmunk	13	253
231	Rochester, NY	raccoon	22	300
236	Rochester, NY	white tailed deer	20	440
232	Rochester, NY	red fox	23	506

228	Rochester, NY	gray squirrel sp	22	1308
288	Saint Louis, MO	flying squirrel sp	2	2
293	Saint Louis, MO	north american river otter	2	2
284	Saint Louis, MO	bobcat	4	4
292	Saint Louis, MO	north american mink	6	9
290	Saint Louis, MO	gray fox	8	21
296	Saint Louis, MO	striped skunk	9	75
299	Saint Louis, MO	woodchuck	14	79
287	Saint Louis, MO	eastern chipmunk	11	81
283	Saint Louis, MO	armadillo	8	224
286	Saint Louis, MO	coyote	27	350
295	Saint Louis, MO	red fox	24	356
285	Saint Louis, MO	cottontail sp	25	581
289	Saint Louis, MO	fox squirrel	28	640
297	Saint Louis, MO	virginia opossum	32	1510
294	Saint Louis, MO	raccoon	35	2978
298	Saint Louis, MO	white tailed deer	25	3037
291	Saint Louis, MO	gray squirrel sp	35	7115
256	Salt Lake City, UT	fox squirrel	1	1
260	Salt Lake City, UT	north american badger	1	1
268	Salt Lake City, UT	weasel sp	1	1
269	Salt Lake City, UT	yellow bellied marmot	1	1
250	Salt Lake City, UT	black bear	1	2
259	Salt Lake City, UT	muskrat	2	2
255	Salt Lake City, UT	elk	4	6
261	Salt Lake City, UT	north american beaver	3	8
253	Salt Lake City, UT	cougar	9	10
252	Salt Lake City, UT	cottontail sp	4	11
262	Salt Lake City, UT	north american porcupine	9	13
251	Salt Lake City, UT	bobcat	12	15
265	Salt Lake City, UT	red squirrel	11	36
264	Salt Lake City, UT	red fox	15	53
266	Salt Lake City, UT	rock squirrel	11	63
257	Salt Lake City, UT	moose	27	66
254	Salt Lake City, UT	coyote	31	71
267	Salt Lake City, UT	striped skunk	25	79
263	Salt Lake City, UT	raccoon	31	150
258	Salt Lake City, UT	mule deer	67	570
244	Sanford, FL	gray fox	1	1
239	Sanford, FL	black bear	2	2
243	Sanford, FL	flying squirrel sp	3	3
247	Sanford, FL	red fox	3	14
240	Sanford, FL	bobcat	8	17
241	Sanford, FL	cottontail sp	10	54
242	Sanford, FL	coyote	16	54
238	Sanford, FL	armadillo	16	116
248	Sanford, FL	virginia opossum	16	159
249	Sanford, FL	white tailed deer	13	230
246	Sanford, FL	raccoon	21	316
245	Sanford, FL	gray squirrel sp	26	439

281	Seattle, WA	striped skunk	1	1
276	Seattle, WA	flying squirrel sp	1	2
279	Seattle, WA	north american river otter	2	2
275	Seattle, WA	elk	1	12
274	Seattle, WA	douglas squirrel	5	14
270	Seattle, WA	black bear	3	15
271	Seattle, WA	bobcat	8	15
282	Seattle, WA	virginia opossum	18	195
278	Seattle, WA	mule deer	13	326
273	Seattle, WA	coyote	23	339
272	Seattle, WA	cottontail sp	20	438
280	Seattle, WA	raccoon	28	646
277	Seattle, WA	gray squirrel sp	28	1510
307	Tacoma, WA	fox squirrel	1	1
300	Tacoma, WA	black bear	1	2
310	Tacoma, WA	mountain beaver	1	2
315	Tacoma, WA	weasel sp	5	5
301	Tacoma, WA	bobcat	3	12
305	Tacoma, WA	eastern chipmunk	5	29
316	Tacoma, WA	western chipmunk	5	58
309	Tacoma, WA	jackrabbit sp	9	79
306	Tacoma, WA	elk	5	92
313	Tacoma, WA	striped skunk	8	136
304	Tacoma, WA	douglas squirrel	11	231
314	Tacoma, WA	virginia opossum	31	548
303	Tacoma, WA	coyote	36	574
302	Tacoma, WA	cottontail sp	29	637
311	Tacoma, WA	mule deer	27	879
312	Tacoma, WA	raccoon	40	1333
308	Tacoma, WA	gray squirrel sp	35	2226
321	Urbana, IL	flying squirrel sp	1	1
326	Urbana, IL	north american beaver	2	2
317	Urbana, IL	bobcat	3	3
324	Urbana, IL	muskrat	1	3
325	Urbana, IL	north american badger	1	3
328	Urbana, IL	north american river otter	2	3
333	Urbana, IL	weasel sp	3	3
327	Urbana, IL	north american mink	18	83
330	Urbana, IL	red fox	18	115
331	Urbana, IL	striped skunk	16	160
335	Urbana, IL	woodchuck	16	250
319	Urbana, IL	coyote	31	336
320	Urbana, IL	eastern chipmunk	18	399
322	Urbana, IL	fox squirrel	27	1577
318	Urbana, IL	cottontail sp	31	1582
332	Urbana, IL	virginia opossum	34	1642
334	Urbana, IL	white tailed deer	33	2267
323	Urbana, IL	gray squirrel sp	33	2268
329	Urbana, IL	raccoon	35	2519
182	Washington D.C. metro area	north american mink	2	2

183	Washington D.C. metro area	north american river otter	2	2
179	Washington D.C. metro area	flying squirrel sp	3	6
180	Washington D.C. metro area	gray fox	2	18
177	Washington D.C. metro area	coyote	29	82
188	Washington D.C. metro area	woodchuck	19	105
178	Washington D.C. metro area	eastern chipmunk	21	346
176	Washington D.C. metro area	cottontail sp	30	485
186	Washington D.C. metro area	virginia opossum	45	710
185	Washington D.C. metro area	red fox	75	2422
184	Washington D.C. metro area	raccoon	75	3157
187	Washington D.C. metro area	white tailed deer	69	3349
181	Washington D.C. metro area	gray squirrel sp	73	4872
350	Wilmington, DE	weasel sp	1	1
344	Wilmington, DE	north american river otter	3	8
339	Wilmington, DE	flying squirrel sp	3	9
341	Wilmington, DE	muskrat	2	10
337	Wilmington, DE	coyote	6	16
343	Wilmington, DE	north american mink	8	32
347	Wilmington, DE	red squirrel	2	32
348	Wilmington, DE	striped skunk	13	59
342	Wilmington, DE	north american beaver	7	68
338	Wilmington, DE	eastern chipmunk	6	80
352	Wilmington, DE	woodchuck	19	184
336	Wilmington, DE	cottontail sp	23	431
349	Wilmington, DE	virginia opossum	28	688
346	Wilmington, DE	red fox	29	2161
351	Wilmington, DE	white tailed deer	28	2221
345	Wilmington, DE	raccoon	29	2579
340	Wilmington, DE	gray squirrel sp	29	3898

Social-environmental variables

We calculated two independent variables and included both in all models. First, to represent a gradient of urban intensity we calculated the percent impervious cover within 1 km of each site from the 2019 National Land Cover Database imperviousness dataset (Dewitz and U.S. Geological Survey, 2021). Second, we determined if each site was within 500 m of a gentrifying Census tract. To quantify gentrification across a wide range of cities we modified a two-step process described by Chapple et al. (2017). For the first step, we identified Census tracts that were vulnerable to gentrification in 2010 as tracts with at least 500 residents and two of these three qualities: 1) a median income less than the city's average income, 2) a proportion of college-educated residents less than the city average, and 3) a proportion of nonwhite residents greater than the city average. To calculate gentrification vulnerability we used the 2010 US decennial Census data via the tidycensus package in R v 4.2.0 (Walker 2022, R Core Team 2022). For the second step, we used the 2019 American Community Survey (U.S. Census Bureau 2012) data to determine if a vulnerable Census tract became gentrified. Here, vulnerable tracts from the first step were identified as gentrified if they experienced a greater increase in median income between 2010 and 2019 than the average change across a city–after correcting for inflation–as well as one of two qualities: a change in college-educated residents or a change in the proportion of non-Hispanic white residents between 2010 and 2019 that exceeded the average change across the city. For additional details and summaries regarding this gentrification metric see the "Additional gentrification metric details" section of the supplemental material.

Associations between gentrification and our social-environmental variables

Among cities, on average, 25% (sd = 11%) of camera sites were within 500m of a gentrified Census tract. At sites near gentrified Census tracts, 46% (sd = 20%) of land cover was impervious, on average, while sites not near gentrified Census tracts had an average of 25% (sd = 21%) impervious cover. Within cities, Urbana, Illinois had the lowest percent of sites within 500m of a gentrified Census tract (3%) and Phoenix, Arizona had the highest (50%). See Supplemental Material X1 for additional information on within-city variation in impervious cover and maps of gentrified and non-gentrified Census tracts.

With respect to the 2019 distribution of the variables we used to quantify gentrification across cities, the median per capita income of gentrified Census tracts (mean = $68,785, sd = $28,193) was roughly $30,000 less than non-gentrified Census tracts (mean = $98,678, sd = $50,777). The proportion of non-Hispanic white residents living in gentrified Census tracts (mean = 0.28, sd = 0.26) was lower than non-gentrified Census tracts (mean = 0.48, sd = 0.30), and the proportion of people with a college degree in gentrified Census tracts (mean = 0.34, sd = 0.18) was slightly lower than non-gentrified Census tracts (mean = 0.48, sd = 0.23). Thus, gentrified Census Tracts still have lower incomes, fewer non-Hispanic white residents, and fewer college educated residents than non-gentrified Census Tracts. However, gentrified Census tracts saw greater than average shifts in these variables over time, such that the residents living there have become whiter, richer, and more educated.

Gentrification may also be associated with an increase in urban greenspace. As such, we quantified whether gentrified Census tracts had a greater increase in the proportion of greenspace (i.e., developed, open space from NLCD data) over the same time frame we used to quantify gentrification (i.e., 2010 to 2019). We did not find this to be true. After averaging the proportional increase in urban greenspace across gentrified and not-gentrified census tracts in each city, the among-city range in both types of Census tracts was effectively zero (min = -0.01, max = 0.00).

Brief overview of Statistical modeling

We used a meta-analytic approach to quantify associations between gentrification and impervious cover and patterns of alpha and beta diversity across U.S. cities, using a Bayesian approach for all models (see following sections for more thorough explanation of our three statistical models). However, unlike more-common meta-analyses, which must contend with issues of publication bias that can distort results (Nakagawa et al. 2022), our analysis used all available UWIN data to parameterize both alpha- and beta diversity models, resulting in a more unbiased and data-driven evaluation of our hypothesis.

To do so, we first fitted a Bayesian multi-city, multi-species occupancy model that included a first-order autoregressive term to account for repeat sampling across primary sampling periods within each city (Sutherland et al. 2016, Royle and Dorazio 2008, Magle et al. 2021). This model had three separate logit-linear predictors: one to indicate a species presence within a city's species pool, one for site-level occupancy, and one for site-level detection probability. Following Magle et al. (2021), we included the distance of each city to the known margin of a species' geographic range in the first linear predictor, with positive and negative numbers respectively indicating cities within and outside a species range. Range data came from IUCN red list data (IUCN 2020). For site-level occupancy and detection, we included impervious cover, gentrification, and the interaction between the two as slope terms in the model. All species-level parameters shared information among species and cities via their random effect structure. Following a 1,000 step adaptation phase and a 125,000 step burn-in, we sampled the posterior 120,000 times across 4 chains. We thinned chains by 3 for a total of 40,000 posterior samples. We assessed model convergence through a visual inspection of traceplots and ensured Gelman-Rubin diagnostics were < 1.10 (Gelman et al., 2013). Following model convergence, we simulated species occupancy at each site across the entire study area from 5000 random samples of the occupancy model's posterior distribution.

For the alpha diversity model we calculated 1) the expected species richness at each site and 2) the standard deviation in this estimate across the 5,000 posterior samples. To limit the effect of individual years on these estimates we calculated species richness at a site across all possible sampling periods. This resulted in one estimate per site across cities. We then fitted a varying intercept, varying slope log-linear model to these data, which treated species richness as the response variable but also incorporated the associated uncertainty

in this estimate (Kery and Royle citation). Intercept and slope terms were treated as city-level random effects. We included impervious cover, gentrification, and the interaction between the two as covariates.

For the beta diversity model we calculated 1) pairwise community dissimilarity between pairs of sites within each city (i.e., Sørensen's dissimilarity index) and 2) the standard deviation in this estimate across the 5,000 posterior samples (Legendre & Legendre 2012). Like the alpha diversity model, beta diversity estimates were made across all primary sampling periods. We then fitted a varying intercept, varying slope generalized dissimilarity model to these data, which treated pairwise dissimilarity as the response variable (GDM CITATION). This model used a clog link function and had an inverse link function of $1 - \exp(-\mu)$, where μ is the linear predictor for one data point. Similar to the alpha diversity model, the beta diversity model incorporated the associated uncertainty in the beta diversity estimate. Intercepts and slopes were treated as city-level random effects. Because community composition may be more similar in nearby sites, we controlled for geographic distance between site pairs by including it as a covariate. We also included differences in impervious cover and gentrification between sites as covariates. However, because this model uses I-spline basis functions to incorporate possible non-linear responses we could not include an interaction between gentrification and impervious cover in this model (GDM CITATION). See the occupancy, alpha and beta diversity models section of the supplemental material.

The multi-city multi-species autologistic occupancy model

This model is almost exactly the same model as we had used in Magle et al. (2022). For s in $1, ..., S$ species and c in $1, ..., C$ cities, π_{sc} is the probability species s is within city c. Futher, let x_{sc} be a Bernoulli random variable that equals 1 if the species is within that city and is otherwise zero such that $x_{sc} \sim \text{Bernoulli}(\pi_{sc})$. We made π_{sc} a function of one covariate–the distance a city is from the known edge of a species extent–using the logit link. This covariate was positive if a city was within a species extent and negative if it was outside. We compiled range information from IUCN red list data (IUCN, 2020). Thus the linear predictor for this level of the model was

$$\text{logit}(\pi_{sc}) = \boldsymbol{d}_s \boldsymbol{h}_c$$

where $\boldsymbol{d}_s$ is a vector of species-specific covariates while $\boldsymbol{h}_c$ is a vector of conformable regression coefficients where the leading element is 1 to accomodate the model intercept.

As the first level of the model estimates a species presence at the city-level, the next level estimates species presence within cities conditional on their presence in a city. Given that the number of sites and sampling periods varies across cities, we add a city subscript to define i_c in $1, ..., I_c$ sites and t_c in $1, ..., T_c$ sampling periods. However, for simplicity we drop these specific subscripts while we explain the model. Additionally, let z_{scit} be a Bernoulli random variable and ψ_{scit} be the probability of occupancy. As such, $z_{scit} \sim \text{Bernoulli}(\psi_{scit} x_{sc})$. As with the previous level of the model, ψ_{scit} can be made a function of covariates via the logit link. As a depature from the Magle et al. (2022) parameterization, we added a first-order autologistic term to account for any temporal dependence in occupancy status between adjacent sampling periods within a city. Thus, for the first time period in a city, the logit-linear predictor was

$$\text{logit}(\psi_{scit=1}) = \boldsymbol{\beta}_{sc} \boldsymbol{f}_{ci}$$

where $\boldsymbol{\beta}_{sc}$ is a vector of species and city-specific parameters and $\boldsymbol{f}_{ci}$ is a vector of conformable covariates whose first value is 1 for the model intercept. After the first sampling season, we added our autologistic term

$$\text{logit}(\psi_{scit}) = \boldsymbol{\beta}_{sc} \boldsymbol{f}_{ci} + \theta_{sc} z_{scit-1}, \text{ for t} > 1.$$

For the data model, y_{scit} was the number of days species s was detected at city c and site i on sampling season t. Given j_{cit} days of sampling, we assumed y_{scit} is a binomial random variable conditional on species presence

$$y_{scit} | z_{scit} \sim \text{Binomial}(j_{cit}, \rho_{scit} z_{scit})$$

where ρ_{scit} is the daily probability of detection that can be made a function of covariates with the logit link,

$$\text{logit}(\rho_{scit}) = \boldsymbol{\alpha}_{sc}\boldsymbol{g}_{ci}$$

where $\boldsymbol{\alpha}_{sc}$ is a vector of parameters and $\boldsymbol{g}_{ci}$ is a vector of conformable covariates where the leading value is 1 to accommodate the intercept.

Given that some species occur across multiple cities, there are multiple levels in which species could partially share information. At the top-level of the model we have the simplest hierarchical parameterization for parameters associated to π_{sc}, namely that there is a community mean for each parameter of which species-level coefficients vary around. We show this for the model intercept with the understanding that the same parameterization applies to all logit-scale covariates in this part of the model.

$$\begin{aligned}
\bar{d}_{0s} &\sim \text{Cauchy}(0, 2.5) \\
\sigma_{d_0} &\sim \text{Inv-Gamma}(1, 1) \\
d_{0s} &\sim \text{Normal}(\bar{d}_{0s}, \sigma_{d_0})
\end{aligned}$$

For the rest of the latent state model we add an additional hierarchical level to the model. However, this parameterization also aligns with the data model, and as such so we only describe it here once for the model intercept of the latent-state model. For example, for the model intercepts we begin with a community-level average among species and cities ($\bar{\beta}_0$). This parameter partially informs a species-level average among cities ($\bar{\beta}_{0s}$), which then informs species-specific coefficients in all cities (β_{0sc}).

$$\begin{aligned}
\bar{\beta}_0 &\sim \text{Cauchy}(0, 2.5) \\
\sigma_{\beta_0} &\sim \text{Inv-Gamma}(1, 1) \\
\bar{\beta}_{0s} &\sim \text{Normal}(\bar{\beta}_0, \sigma_{\beta_0}) \\
a_{\beta_0} &\sim \text{Uniform}(0, 10) \\
b_{\beta_0} &\sim \text{Uniform}(0, 10) \\
\sigma_{\beta_{0s}} &\sim \text{Inv-Gamma}(a_{\beta_0}, b_{\beta_0}) \\
\beta_{0sc} &\sim \text{Normal}(\bar{\beta}_{0s}, \sigma_{\beta_{0s}})
\end{aligned}$$

We added the hyperparameters for the shape (a_{β_0}) and rate (b_{β_0}) of the Inv-Gamma distribution to account for the fact that some cities may only have one sampling period of data. Note that the above parameterization also applies to the autologistic term of the model (θ_{sc}).

Finally, the latent state and data model included one other set of parameters to account for variation in occupancy or detectability across sampling seasons. As we have already added hierarchical structure via the centered parameterization of the other model parameters, we usd a non-centered parameterization here for this level of variability. Again, we show this for the latent state, but with a swapping of subscripts this could readily be applied to the data model as well.

$$\begin{aligned}
a_{\psi} &\sim \text{Uniform}(0, 10) \\
b_{\psi} &\sim \text{Uniform}(0, 10) \\
\sigma_{\psi c} &\sim \text{Inv-Gamma}(a_{\psi}, b_{\psi}) \\
\beta_{sct} &\sim \text{Normal}(0, \sigma_{\psi c})
\end{aligned} \tag{1}$$

With this parameterization, β_{sct} is a difference term that represents the logit-scale difference in occupancy for species s at city c from their average β_{0sc} (i.e., the model intercept). Again, like with the other parameters in this part of the model, we used hyperparameters for the Inv-Gamma distribution because not every city had more than one season of data.

The alpha diversity meta-analytic model

From our occupancy model we created a posterior distribution for the latent state of each species at each site across all cities (z_{scit}). From this, we derived two quantities for this model:

1. The mean expected species richness at each site across all sampling periods (r_{ci}). To do so, we calculated the number of unique species detected in city c and site i across the t sampling seasons and took the median across 5000 posterior samples.
2. The standard deviation of the first quantity across those 5000 posterior samples (σ_{ci}). This quantifies our level of uncertainty with the first estimate.

Following this, let $\boldsymbol{\beta}_c$ be a vector of city-specific regression coefficients and $\boldsymbol{x}_{ci}$ be a vector of city and site specific covariates where the leading element is 1 to account for the intercept. Within the linear predictor we also added an additional residual variation term, ϵ_{ci}, which was given a $\sim$ Inv-Gamma$(1, 1)$ prior. Thus, the log-linear predictor was

$$\log(\mu_{sci}) = \boldsymbol{\beta}_c \boldsymbol{x_{ci}} + \epsilon_{ci}$$

and following Kery and Royle (YEAR), we accounted for variability in the response variable with an additional level of the model

$$r_{ci} \sim \text{Normal}(\mu_{sci}, \sigma_{ci})$$

We treated the intercept and slope terms as city-level random effects. For example, the prior for the model intercept was

$$\begin{aligned}
\bar{\beta}_0 &\sim \text{Cauchy}(0, 2.5) \\
\sigma_{\beta_0} &\sim \text{Inv-Gamma}(1, 1) \\
\beta_{0c} &\sim \text{Normal}(\bar{\beta}_0, \sigma_{\beta_0})
\end{aligned}$$

and the same specification was also applied to the slope terms as well (though not described here).

The beta diversity meta-analytic model

From our occupancy model, we created a posterior distribution for the latent state of each species at each site across all cities (z_{scit}). From this, we derived three quantities:

1. The mean pairwise Sorensen dissimilarity between pairs of sites within each city across all sampling periods (v_{cik}, where the subscript k denotes one of the sites in city c that is not the ith site). To do so, we calculated the number of unique species detected in city c and site i across the t sampling seasons. Following this, we calculated the Sorensen dissimilarity metric among all pairs of sites within each city using `vegan` in `R` across 5000 posterior samples. Finally, we took the median across all posterior samples for each site-pair
2. The standard deviation of the first quantity across those 5000 posterior samples (σ_{cik}). This quantifies our level of uncertainty with the first estimate.
3. The mean expected number of unique species between a site-pair (w_{cik}).

To estimate pairwise dissimilarity as a function of covariates we modified a generalized dissimilarity model to account for parametetric uncertainity of the response variable v_{cik} (GDM citation). To do so, GDMs estimate the relationship between dissimilarity and environmental or spatial differences between pairs of sites with a clog link (Mokany et al. 2022):

$$d_{cik} = 1 - \exp(-\eta_{cik})$$

where d_{cik} is the biological dissimilarity between sites i and k within city c and η_{cik} is the predicted ecological distance between (i.e., the linear predictor). Given p in 1,..,P covariates, the ecological distance between sites is

$$\eta_{cik} = b_0 + \sum_{p=1}^{P} |f_p(x_{cip}) - f_p(x_{ckp})|$$

where b_0 is the model intercept (i.e., the expected pairwise dissimilarity between sites with identical environments). Covariates are further transformed within GDMs which 1) uses I-spline basis functions (Ramsay, 1988) and 2) constrains slope terms to be non-negative. Doing so allows the effect of each covariate to non-linearly vary while also ensuring that beta diversity increases monotonically as sites are more different from one another (a core assumption of this model). More specifically, the I-spline basis function for predictor p with 3 basis functions (the default used for GDMs) is

$$fp(x_{cip}) = \sum_{j=1}^{3} a_{cpj} I_{pj}(x_{cip})$$

where a_{cpj} is a non-negative coefficient for the jth I-spline and I_{pj} is the jth I-spline of the covariate x_{cip}. For our own model, the binary gentrification status of site-pairs was not sent through an I-spline basis function. Instead, we used a dummy variable that took the value of 1 if a pair of sites differed in their gentrification status and was otherwise 0. Regardless, all slope terms were constrained to be non-negative. Thus, given η_{cik} and the total number of species between site pairs (w_{cik}), the first level of our model is

$$\begin{aligned} d_{cik} &= 1 - \exp(-\eta_{cik}) \\ \sigma_{cik} &= \sqrt{\frac{d_{cik} - (1 - d_{cik})}{w_{cik}}} \\ \mu_{cik} &\sim \text{Half-Normal}(d_{cik}, \sigma_{cik}) \end{aligned} \tag{2}$$

where σ_{cik} is the binomial variance function (Mokany et al. 2022) and the half-Normal is constrained to be non-negative. Following this, we account for variation in the measurement of our response variable

$$v_{cik} \sim \text{Half-Normal}(\mu_{cik}, \sigma_{cik})$$

where again σ_{cik} is measured based on the output of the occupancy model and provided as data to this model.

We treated all coefficients in the linear predictor as city-level random effects. For example for the model intercept the prior specification would be $b_c \sim \text{Half-Normal}(\bar{b}, \sigma_b)$ where $b \sim \text{Half-Normal}(0, 10)$ and $sigma_b \sim \text{Inv-Gamma}(1, 1)$. The Half-Normal distributions ensure that the coefficients will be non-negative.

Additional gentrification metrics

As previously stated we used a slightly modified version of the gentrification metric proposed by Chapple et al. (2017). This metric used a two-step process to identify gentrification. First, for an area to be gentrifying, it must be vulnerable to gentrification at the start of the study (in this case that is 2010). For our version of this metric a census tract to be vulnerable to gentrification it must:

1. Have had at least 500 residents in year 2010.
2. Have had at least two of these three qualities

a. The median income of residents in the census tract must be lower than the city's average income.
b. The proportion of college-educated residents in the census-tract must be lower than the proportion of college-educated residents across the city.
c. The proportion of nonwhite residents in the census tract must be greater than the proportion of nonwhite residents across the city.

After calculating census tract vulnerability, we created a 500m radius buffer around each camera trapping location within a city and intersected that buffer with the census tract level vulnerability index. This buffer was chosen to capture the general area around each site that easily fell within the home range of any species in our analysis. For example, a site could be right on the edge of a non-vulnerable census tract that abuts a vulnerable census tract and we would want to identify that location as 'vulnerable.'

Of 999 UWIN sites across 20 cities, 474 (47.4%) were considered vulnerable to gentrification.

Following this, a census tract was considered gentrifying if at the end of the study (in this case that is 2019) a census tract:

1. Was vulnerable to gentrification in 2010.
2. The change in median income was greater than the average change across the city, after correcting for inflation.
3. Had at least one of these two qualities.

a. The change in the proportion of college educated residents was greater than average change across the city.
b. The change in the proportion of non-hispanic white residents was greater than the average change across the city.

Of the 474 sites that were vulnerable to gentrification, about half of them of them were gentrifying (n = 264, 55.7%). However,there is a substantial amount of variation among cities. For example, Urbana, IL only had one of thirty five sites near a gentrifying census tract while Phoenix, AZ had exactly half of their 96 sites in gentrifying areas.

Retrieving the census data

We used the `tidycensus` package in `R` to query census data from the year 2010 and 2019 (CITATION). The 2010 data came from the 10-year decennial census whereas the 2019 data came from the 5-year American Community Survey (ACS).

Across these years we compiled data the aforementioned variables for all census tracts that were within the general area of a UWIN transect. To do so we created a bounding box around the camera trap locations for each city, added a 500m buffer, and then cropped the census data.

Step 1. Determine which areas are vulnerable to gentrification

After cropping the census tracts to an area around a cities sampled location, we calculated the regional median (i.e., median income across census tracts) and identified census tracts that fell below that number in 2010.

Table S2: The number of sites that were above (False) and below (True) the median income across census tracts in 2010. This was used to help determine if sites were vulnerable to gentrification.

City	False	True
Athens, GA	14	14
Bay Area, CA	32	10
Boston, MA	20	3
Chicago, IL	59	44
Denver, CO	19	20
Houston, TX	17	7
Indianapolis, IN	26	15
Iowa City, IA	28	9
Jackson, MS	26	18
Little Rock, AR	17	10
Madison, WI	12	10

Metro LA, CA	32	10
Washington D.C. metro area	42	29
Phoenix, AZ	43	44
Portland, Oregon	18	5
Rochester, NY	10	10
Sanford, FL	14	14
Salt Lake City, UT	83	16
Seattle, WA	19	14
Saint Louis, MO	24	11
Tacoma, WA	18	23
Urbana, IL	19	16
Wilmington, DE	17	12

Following this, we calculated the median educational attainment in 2010 across census tracts, which was calculated similarly to income. We simplified the census data into two categories for educational attainment: those with a college degree and those without a college degree.

Table S3: The number of sites that were above (False) and below (True) the median educational attainment (i.e., college degree) across census tracts in 2010. This was used to help determine if sites were vulnerable to gentrification.

City	False	True
Athens, GA	19	9
Bay Area, CA	34	12
Boston, MA	16	9
Chicago, IL	55	48
Denver, CO	14	25
Houston, TX	19	6
Indianapolis, IN	26	15
Iowa City, IA	15	22
Jackson, MS	29	15
Little Rock, AR	14	13
Madison, WI	12	10
Metro LA, CA	36	6
Washington D.C. metro area	39	34
Phoenix, AZ	46	43
Portland, Oregon	13	10
Rochester, NY	13	10
Sanford, FL	15	13
Salt Lake City, UT	85	14
Seattle, WA	16	17
Saint Louis, MO	23	12
Tacoma, WA	27	14
Urbana, IL	12	23
Wilmington, DE	19	10

We then calculated whether Census tracts had at least 500 people in 2010. The educational attainment data also had information on the number of people in each census tract, so we used that to create a binary metric for whether or not a census tract in 2010 had at least 500 people living in them. Of the 8133 census

tracts across all cities, only 114 of them had fewer than 500 residents.

The final metric we obtained to determine the vulnerability of Census tracts was whether the proportion of non-hispanic white people living there was lower than the regional median.

Table S4: The number of sites near Census tracts that had more (False) or less (True) than the regional median of non-hispanic white residents in 2010. This was used to help determine if sites were vulnerable to gentrification.

City	False	True
Athens, GA	15	13
Bay Area, CA	29	17
Boston, MA	17	10
Chicago, IL	57	46
Denver, CO	21	18
Houston, TX	16	9
Indianapolis, IN	26	15
Iowa City, IA	19	18
Jackson, MS	30	14
Little Rock, AR	20	9
Madison, WI	12	10
Metro LA, CA	41	2
Washington D.C. metro area	42	33
Phoenix, AZ	40	52
Portland, Oregon	15	8
Rochester, NY	13	10
Sanford, FL	17	11
Salt Lake City, UT	85	14
Seattle, WA	19	14
Saint Louis, MO	21	14
Tacoma, WA	27	14
Urbana, IL	21	14
Wilmington, DE	9	20

Finally, after combining these metrics we can arrive at the number of sites that were vulnerable to gentrification in 2010.

Table S5: The number of sites that were (True) and were not (False) vulnerable to gentrification in 2010.

City	False	True
Athens, GA	11	17
Bay Area, CA	32	16
Boston, MA	15	12
Chicago, IL	43	60
Denver, CO	11	28
Houston, TX	16	9
Indianapolis, IN	23	18
Iowa City, IA	24	13
Jackson, MS	23	21
Little Rock, AR	19	10
Madison, WI	5	17

Metro LA, CA	35	10
Washington D.C. metro area	31	44
Phoenix, AZ	33	63
Portland, Oregon	13	10
Rochester, NY	11	12
Sanford, FL	13	15
Salt Lake City, UT	80	19
Seattle, WA	18	15
Saint Louis, MO	21	14
Tacoma, WA	24	17
Urbana, IL	15	20
Wilmington, DE	12	17

Step 2. Determine which vulnerable Census tracts gentrified

This step here required us to compare Census tracts over time (i.e., between 2010 and 2019). However, Census tracts are not constant and are regularly redrawn. As a result, it can be difficult to make a 1 to 1 comparison of Census tracts over time. To address this we used areal interpolation. To do so we first rasterized the 2010 census data at a 500m resolution. Second, we joined the 2019 Census tracts to these data and took the spatial average (i.e., weighted unions by their area). For example, if Census tracts did not change over time, this would technique would provide a close to direct comparison (i.e., a 2019 census tract would mostly intersect the rasterized values of the same 2010 census tract). If a census tract did change, the 2019 census tract would take the spatial average over the 2010 census tracts it intersected with.

After doing this we calculated the median change in income and educational attainment. We also calculated if the proportion of non-hispanic white residents in census tracts increased more than the regional median increase (i.e., more non-hispanic white people moved in than average).

Here is a table that shows how many sites are above (TRUE) and below (FALSE) the average change in in educational attainment.

Table S6: The number of sites where the increase in educational attainment (i.e., a college degree) between 2010 and 2019 was (True) and was not (False) greater than the city average.

City	False	True
Athens, GA	15	13
Bay Area, CA	27	19
Boston, MA	18	7
Chicago, IL	56	48
Denver, CO	21	18
Houston, TX	14	11
Indianapolis, IN	16	25
Iowa City, IA	14	23
Jackson, MS	20	24
Little Rock, AR	18	9
Madison, WI	12	10
Metro LA, CA	27	15
Washington D.C. metro area	45	29
Phoenix, AZ	53	34
Portland, Oregon	15	8
Rochester, NY	7	16
Sanford, FL	9	19
Salt Lake City, UT	79	20

Seattle, WA	16	17
Saint Louis, MO	16	19
Tacoma, WA	24	17
Urbana, IL	26	9
Wilmington, DE	18	11

Table S7: The number of sites that where the change in the proportion of non-hispanic white residents was greater than the city average between 2010 and 2019.

City	False	True
Athens, GA	18	10
Bay Area, CA	27	19
Boston, MA	12	13
Chicago, IL	66	38
Denver, CO	22	17
Houston, TX	16	9
Indianapolis, IN	19	22
Iowa City, IA	20	17
Jackson, MS	26	18
Little Rock, AR	18	9
Madison, WI	10	12
Metro LA, CA	32	11
Washington D.C. metro area	42	32
Phoenix, AZ	33	54
Portland, Oregon	16	7
Rochester, NY	17	6
Sanford, FL	16	12
Salt Lake City, UT	62	37
Seattle, WA	10	23
Saint Louis, MO	7	28
Tacoma, WA	18	23
Urbana, IL	8	27
Wilmington, DE	17	12

For income, in addition to areal interpolation we adjusted for inflation. To do so we used the U.S. Bureau of Labor Statistics inflation calculator to determine how much the price of $1 has changed between January 2010 and January 2019 (it is $1.17). Thus, we multiplied the dollar values of median housing prices in 2000 by `1.17` before comparing changes in housing prices.

Table S8: The number of sites that do (True) and do not (False) reside in Census tracts where the median income increased more than the regional median.

City	False	True
Athens, GA	17	10
Bay Area, CA	18	21
Boston, MA	14	9
Chicago, IL	57	46
Denver, CO	20	19
Houston, TX	13	11

Indianapolis, IN	19	22
Iowa City, IA	10	27
Jackson, MS	27	17
Little Rock, AR	11	16
Madison, WI	11	10
Metro LA, CA	24	18
Washington D.C. metro area	46	25
Phoenix, AZ	45	40
Portland, Oregon	13	10
Rochester, NY	13	7
Sanford, FL	9	19
Salt Lake City, UT	39	60
Seattle, WA	20	13
Saint Louis, MO	12	23
Tacoma, WA	11	30
Urbana, IL	24	11
Wilmington, DE	19	9

After compiling these metrics we are able to combine them with our gentrification vulnerability values to determine which Census tracts gentrified. Finally, we determined which sites were within 500m of a gentrified Census tract.

Table S9: The number of sites that were vulnerable to gentrification in 2010 but did not gentrify, the number of sites that did gentrify, and the number of sites that were not vulnerable so could not gentrify.

City	Vulnerable but did not gentrify	Gentrified	Not vulnerable so did not gentrify
Athens, GA	13	4	15
Bay Area, CA	6	9	40
Boston, MA	4	8	23
Chicago, IL	26	34	77
Denver, CO	12	16	27
Houston, TX	4	5	21
Indianapolis, IN	5	13	36
Iowa City, IA	10	3	27
Jackson, MS	11	10	33
Little Rock, AR	6	4	23
Madison, WI	12	5	10
Metro LA, CA	2	8	43
Washington D.C. metro area	19	25	56
Phoenix, AZ	15	46	77
Portland, Oregon	4	6	19
Rochester, NY	7	5	16
Sanford, FL	5	10	23
Salt Lake City, UT	9	10	90
Seattle, WA	7	8	26
Saint Louis, MO	5	9	30
Tacoma, WA	4	13	37
Urbana, IL	19	1	16
Wilmington, DE	5	12	24

Map of cities

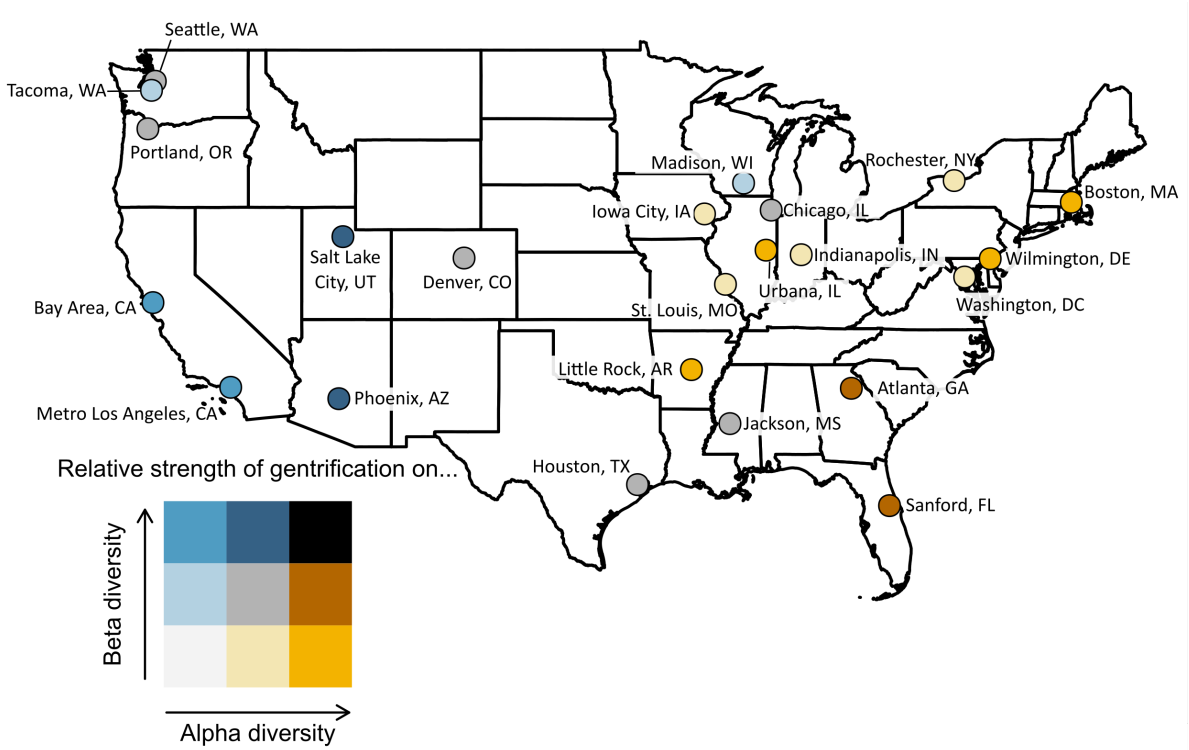

Figure S1: Figure S1. Data from 23 cities were used to assess differences in mammal communities among gentrified and non-gentrified parts of a city. Cities are represented by dots. Dot color illustrates the relative effect of gentrification on alpha and beta diversity at average sites in each city that only vary in their gentrification status. Gentrification had a more pronounced effect on alpha diversity overall. However, gentrification in West Coast cities had a stronger effect on beta diversity, central U.S. cities had a mixture, and East Cost cities had a stronger alpha diversity effect.

City-specific alpha and beta diversity results

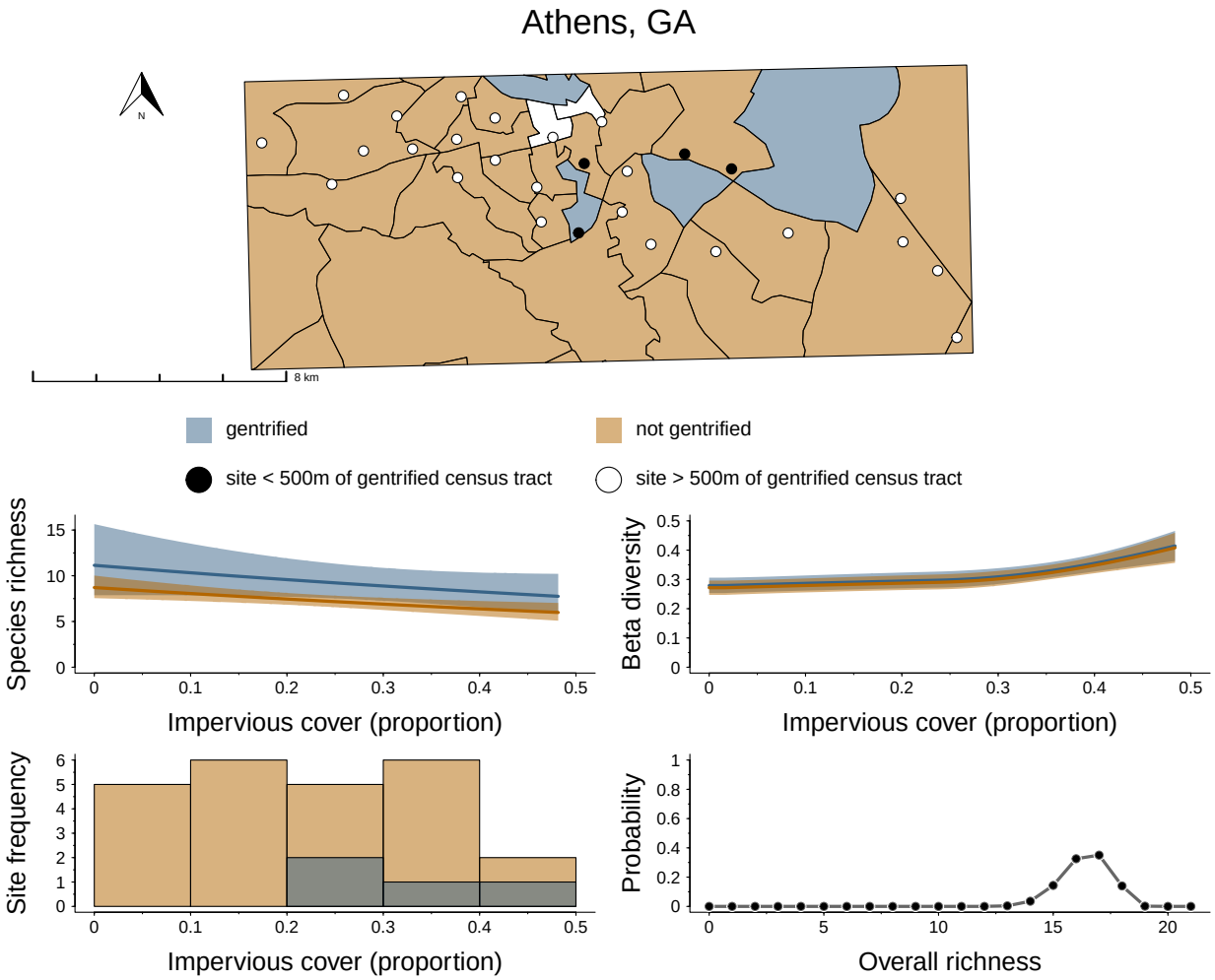

Figure S2. The distribution of gentrifying and non-gentrifying census tracts for Athens, GA as well as the camera trap locations for this city. Below the map are city specific estimates for how alpha diversity (species richness) and beta diversity (Bray-Curtis distance) varies at gentrifying and non-gentrifying sites along a gradient of impervious cover. The lower left histogram shows the proportion of impervious cover at gentrifying and non-gentrifying camera trap locations for Athens, GA. Finally, the lower right plot shows the estimate for total species richness of medium to large mammals for the city (i.e., gamma diversity).

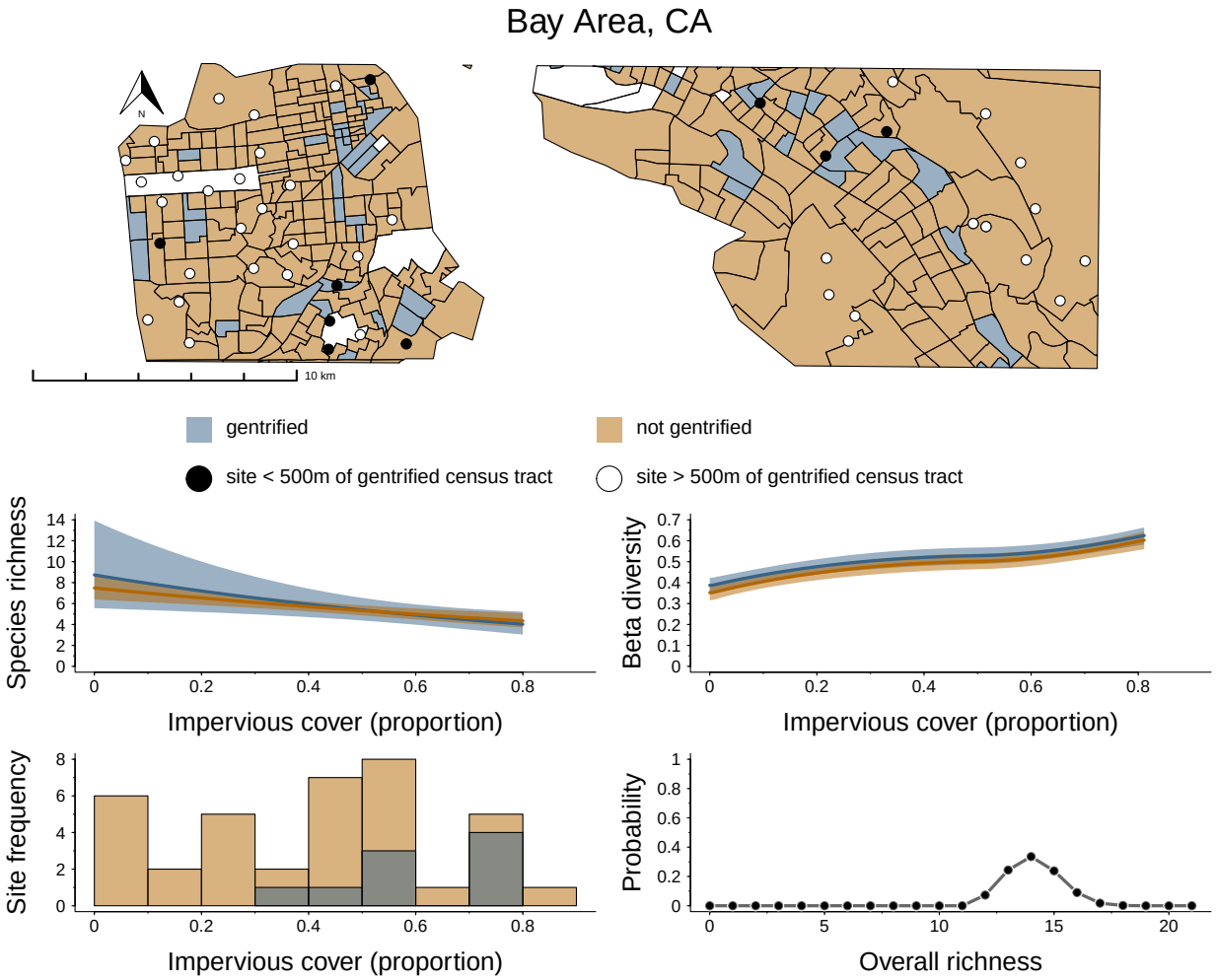

Figure S3. The distribution of gentrifying and non-gentrifying census tracts for Bay Area, CA as well as the camera trap locations for this city. Below the map are city specific estimates for how alpha diversity (species richness) and beta diversity (Bray-Curtis distance) varies at gentrifying and non-gentrifying sites along a gradient of impervious cover. The lower left histogram shows the proportion of impervious cover at gentrifying and non-gentrifying camera trap locations for Bay Area, CA. Finally, the lower right plot shows the estimate for total species richness of medium to large mammals for the city (i.e., gamma diversity).

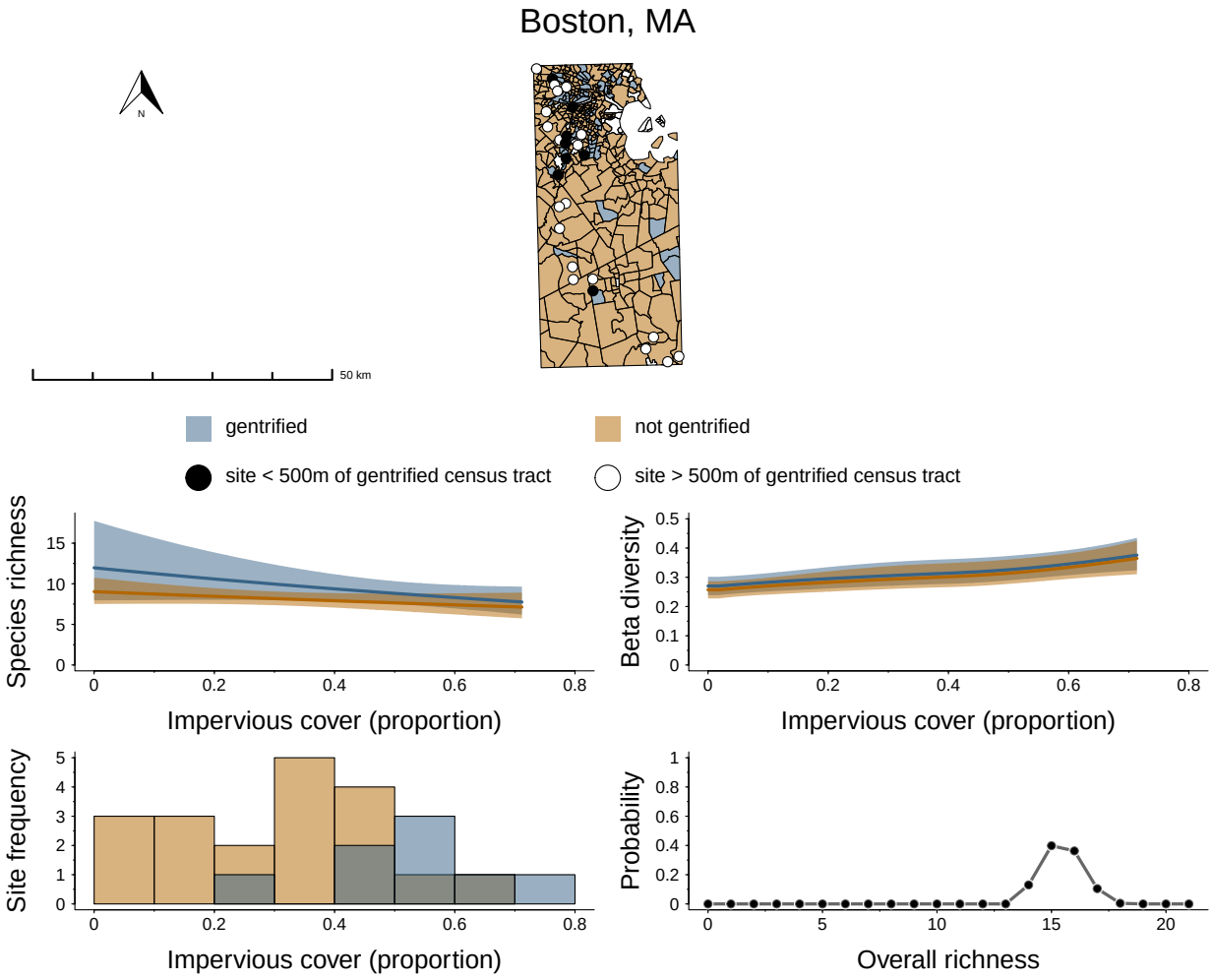

Figure S4. The distribution of gentrifying and non-gentrifying census tracts for Boston, MA as well as the camera trap locations for this city. Below the map are city specific estimates for how alpha diversity (species richness) and beta diversity (Bray-Curtis distance) varies at gentrifying and non-gentrifying sites along a gradient of impervious cover. The lower left histogram shows the proportion of impervious cover at gentrifying and non-gentrifying camera trap locations for Boston, MA. Finally, the lower right plot shows the estimate for total species richness of medium to large mammals for the city (i.e., gamma diversity).

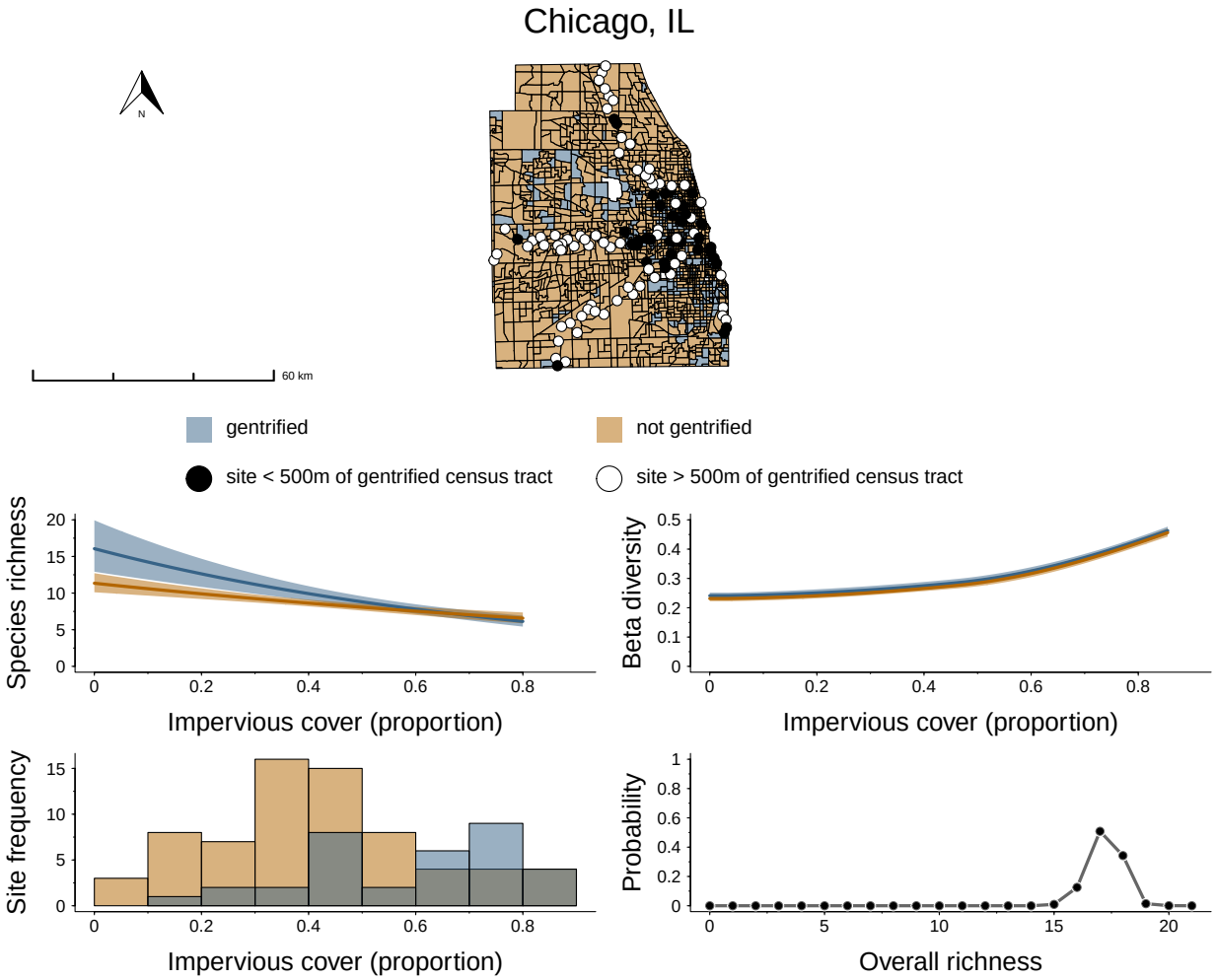

Figure S5. The distribution of gentrifying and non-gentrifying census tracts for Chicago, IL as well as the camera trap locations for this city. Below the map are city specific estimates for how alpha diversity (species richness) and beta diversity (Bray-Curtis distance) varies at gentrifying and non-gentrifying sites along a gradient of impervious cover. The lower left histogram shows the proportion of impervious cover at gentrifying and non-gentrifying camera trap locations for Chicago, IL. Finally, the lower right plot shows the estimate for total species richness of medium to large mammals for the city (i.e., gamma diversity).

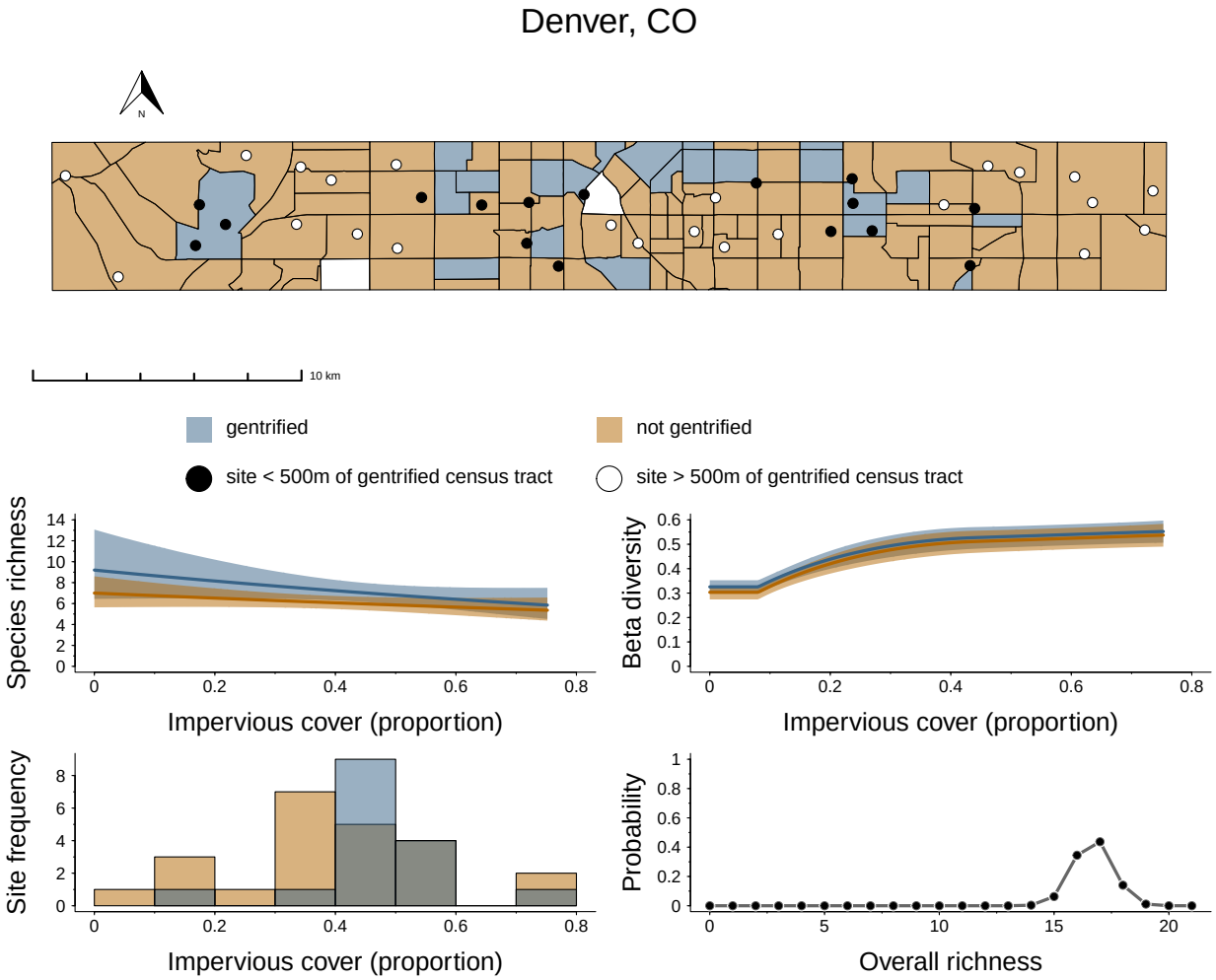

Figure S6. The distribution of gentrifying and non-gentrifying census tracts for Denver, CO as well as the camera trap locations for this city. Below the map are city specific estimates for how alpha diversity (species richness) and beta diversity (Bray-Curtis distance) varies at gentrifying and non-gentrifying sites along a gradient of impervious cover. The lower left histogram shows the proportion of impervious cover at gentrifying and non-gentrifying camera trap locations for Denver, CO. Finally, the lower right plot shows the estimate for total species richness of medium to large mammals for the city (i.e., gamma diversity).

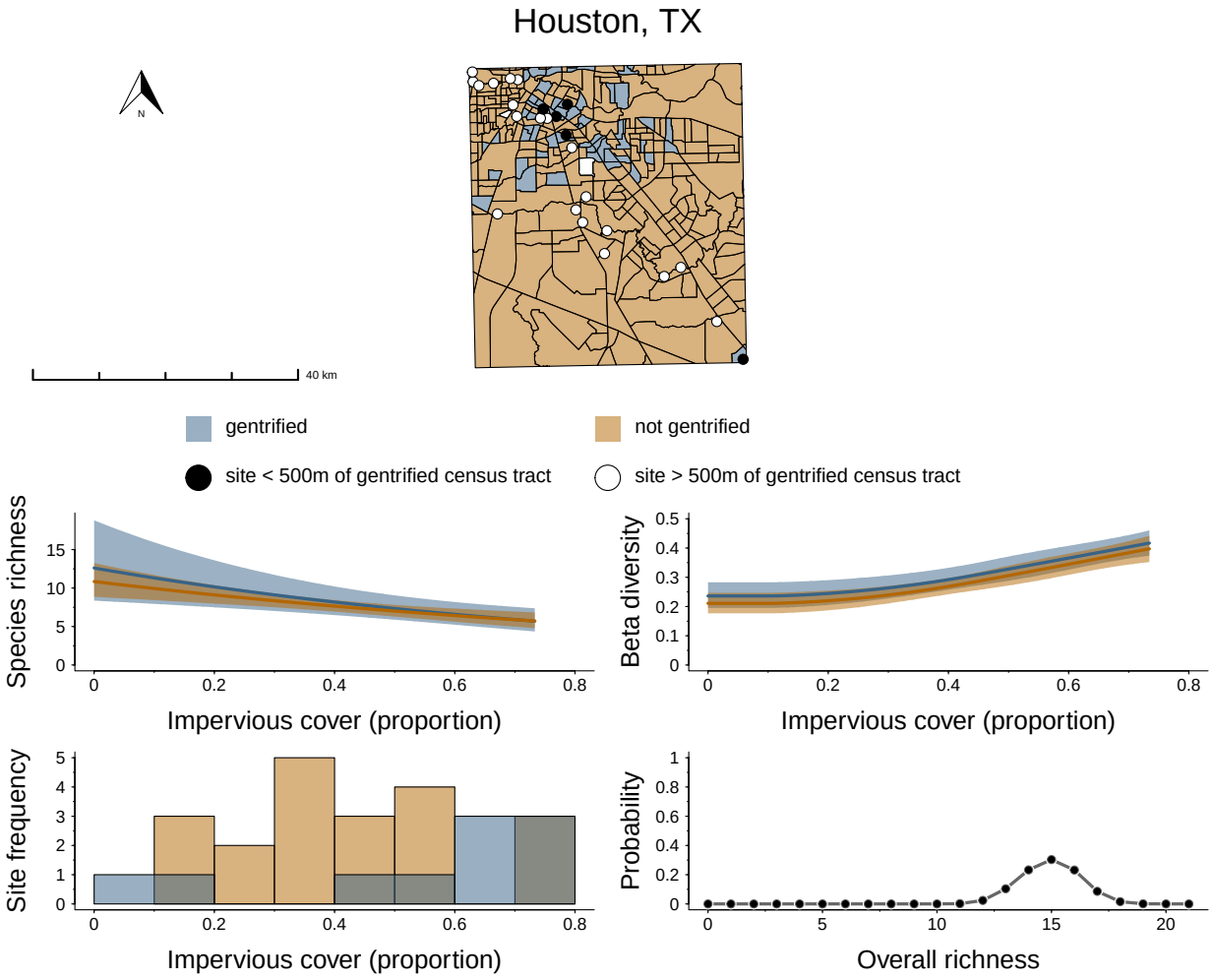

Figure S7. The distribution of gentrifying and non-gentrifying census tracts for Houston, TX as well as the camera trap locations for this city. Below the map are city specific estimates for how alpha diversity (species richness) and beta diversity (Bray-Curtis distance) varies at gentrifying and non-gentrifying sites along a gradient of impervious cover. The lower left histogram shows the proportion of impervious cover at gentrifying and non-gentrifying camera trap locations for Houston, TX. Finally, the lower right plot shows the estimate for total species richness of medium to large mammals for the city (i.e., gamma diversity).

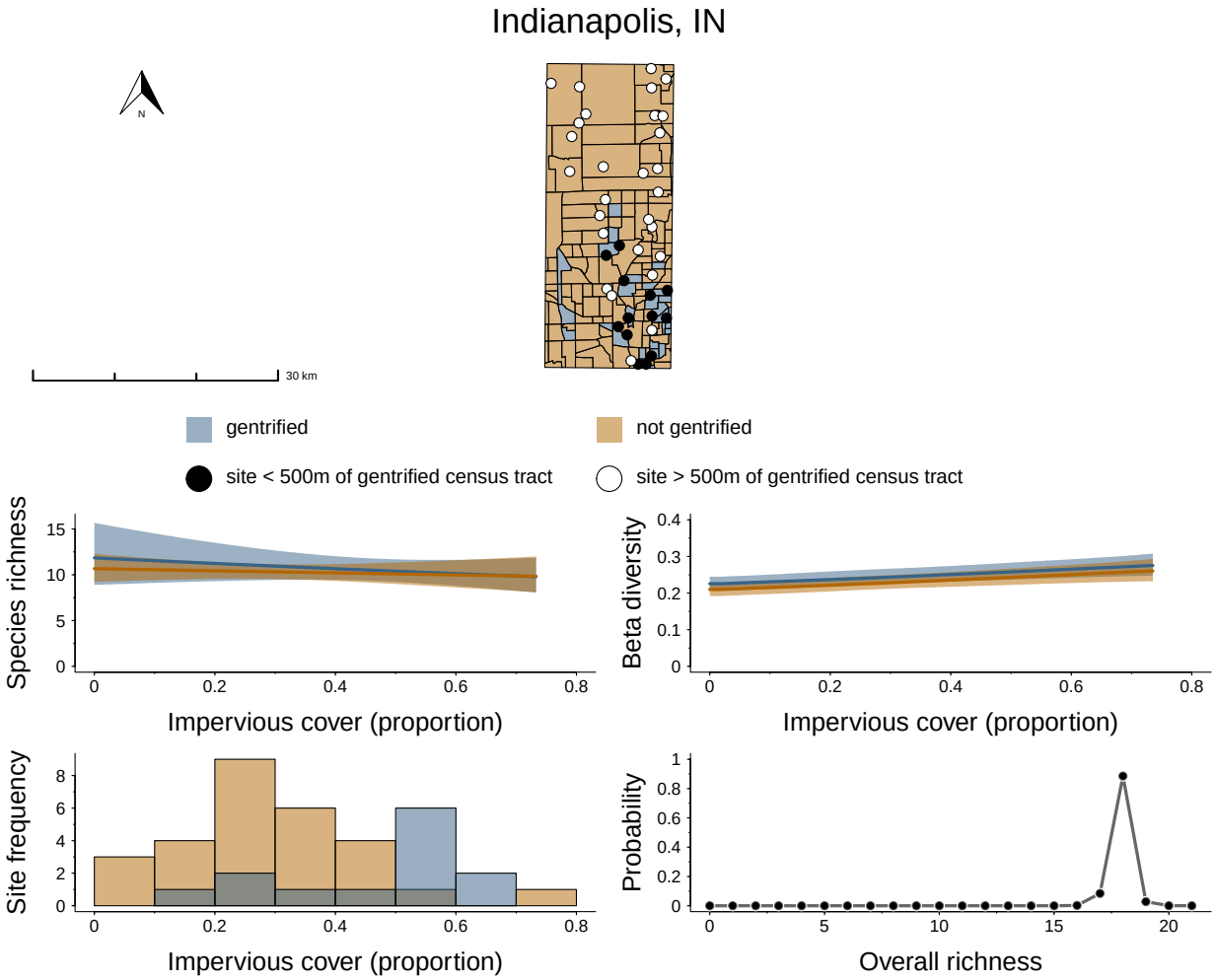

Figure S8. The distribution of gentrifying and non-gentrifying census tracts for Indianapolis, IN as well as the camera trap locations for this city. Below the map are city specific estimates for how alpha diversity (species richness) and beta diversity (Bray-Curtis distance) varies at gentrifying and non-gentrifying sites along a gradient of impervious cover. The lower left histogram shows the proportion of impervious cover at gentrifying and non-gentrifying camera trap locations for Indianapolis, IN. Finally, the lower right plot shows the estimate for total species richness of medium to large mammals for the city (i.e., gamma diversity).

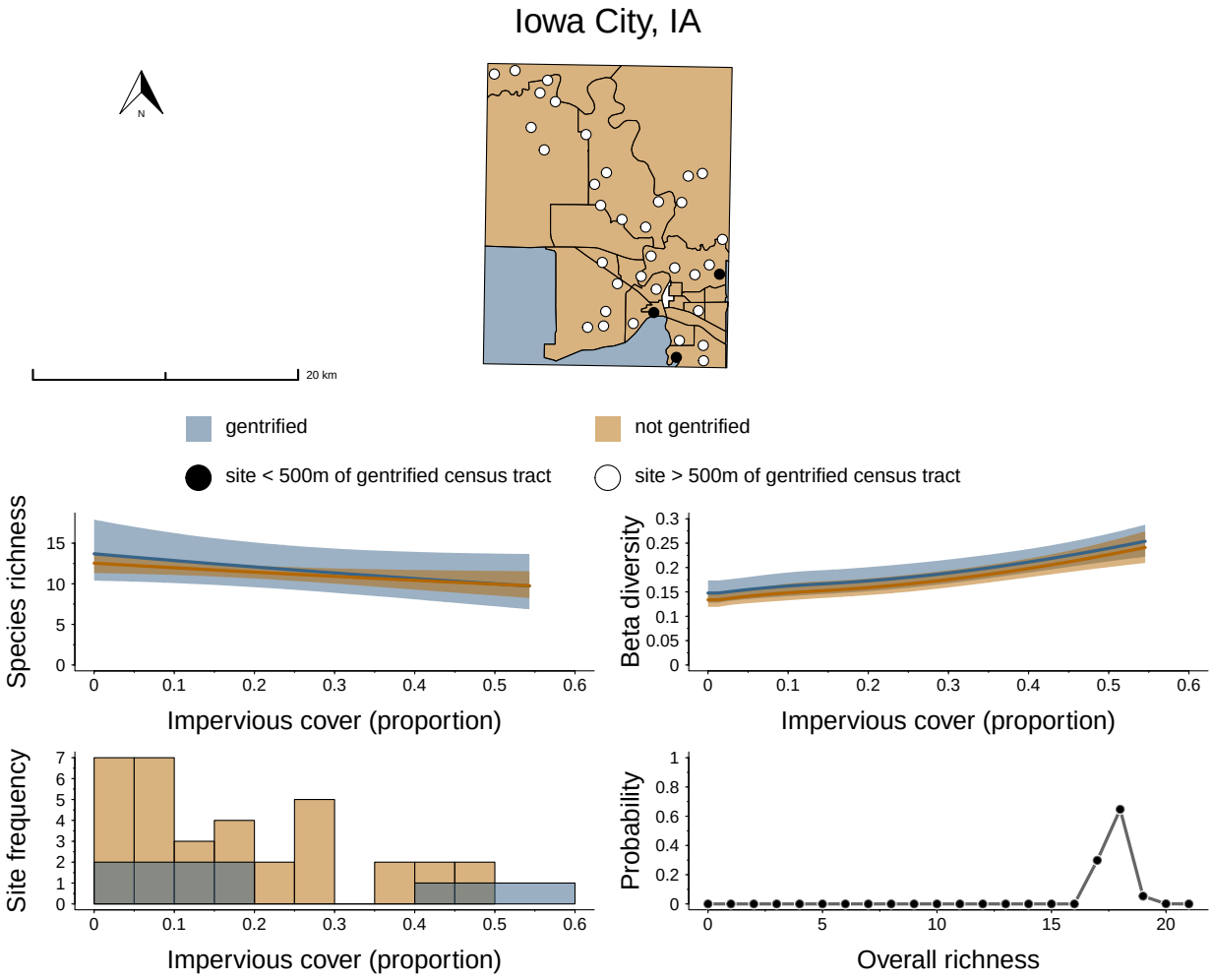

Figure S9. The distribution of gentrifying and non-gentrifying census tracts for Iowa City, IA as well as the camera trap locations for this city. Below the map are city specific estimates for how alpha diversity (species richness) and beta diversity (Bray-Curtis distance) varies at gentrifying and non-gentrifying sites along a gradient of impervious cover. The lower left histogram shows the proportion of impervious cover at gentrifying and non-gentrifying camera trap locations for Iowa City, IA. Finally, the lower right plot shows the estimate for total species richness of medium to large mammals for the city (i.e., gamma diversity).

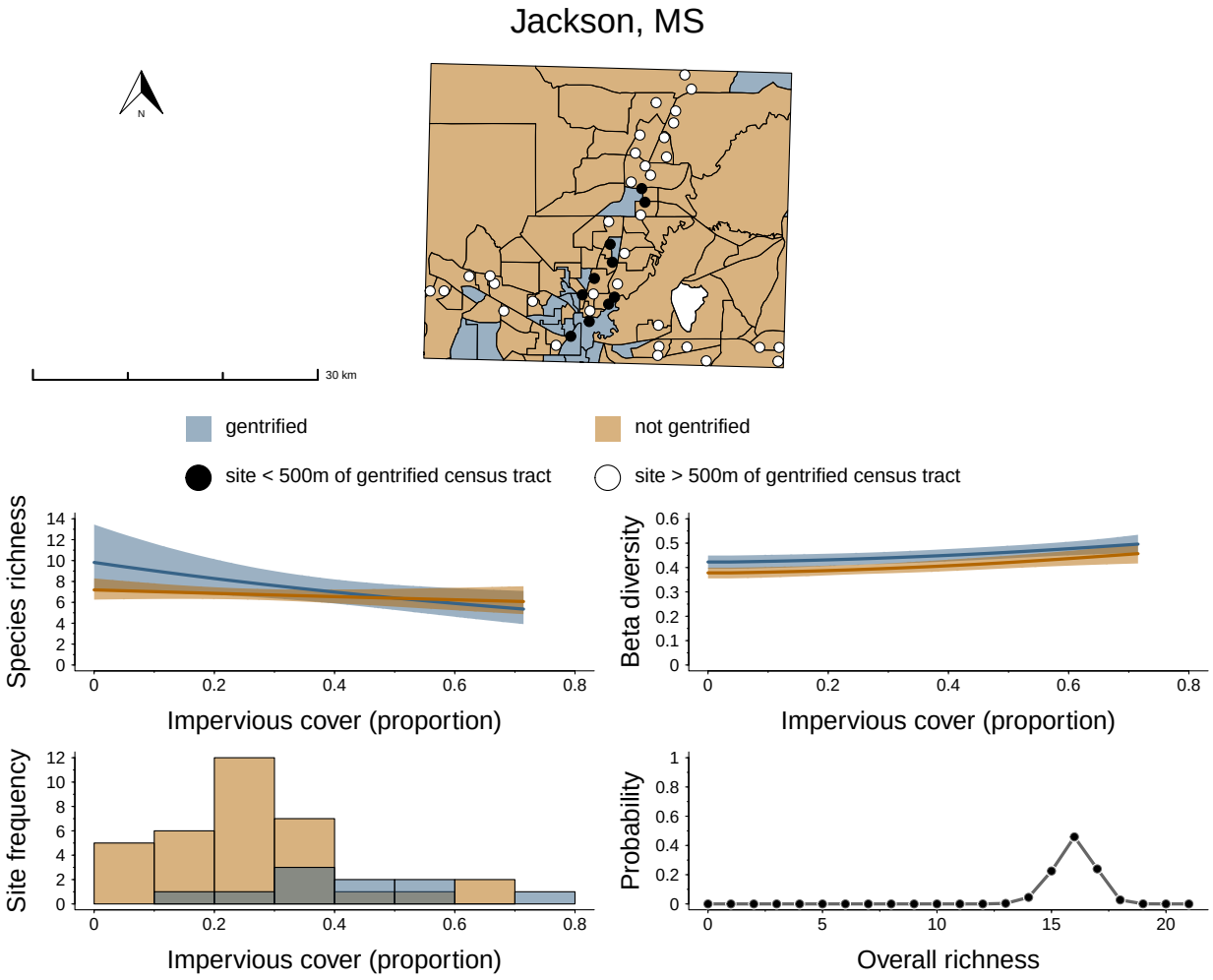

Figure S10. The distribution of gentrifying and non-gentrifying census tracts for Jackson, MS as well as the camera trap locations for this city. Below the map are city specific estimates for how alpha diversity (species richness) and beta diversity (Bray-Curtis distance) varies at gentrifying and non-gentrifying sites along a gradient of impervious cover. The lower left histogram shows the proportion of impervious cover at gentrifying and non-gentrifying camera trap locations for Jackson, MS. Finally, the lower right plot shows the estimate for total species richness of medium to large mammals for the city (i.e., gamma diversity).

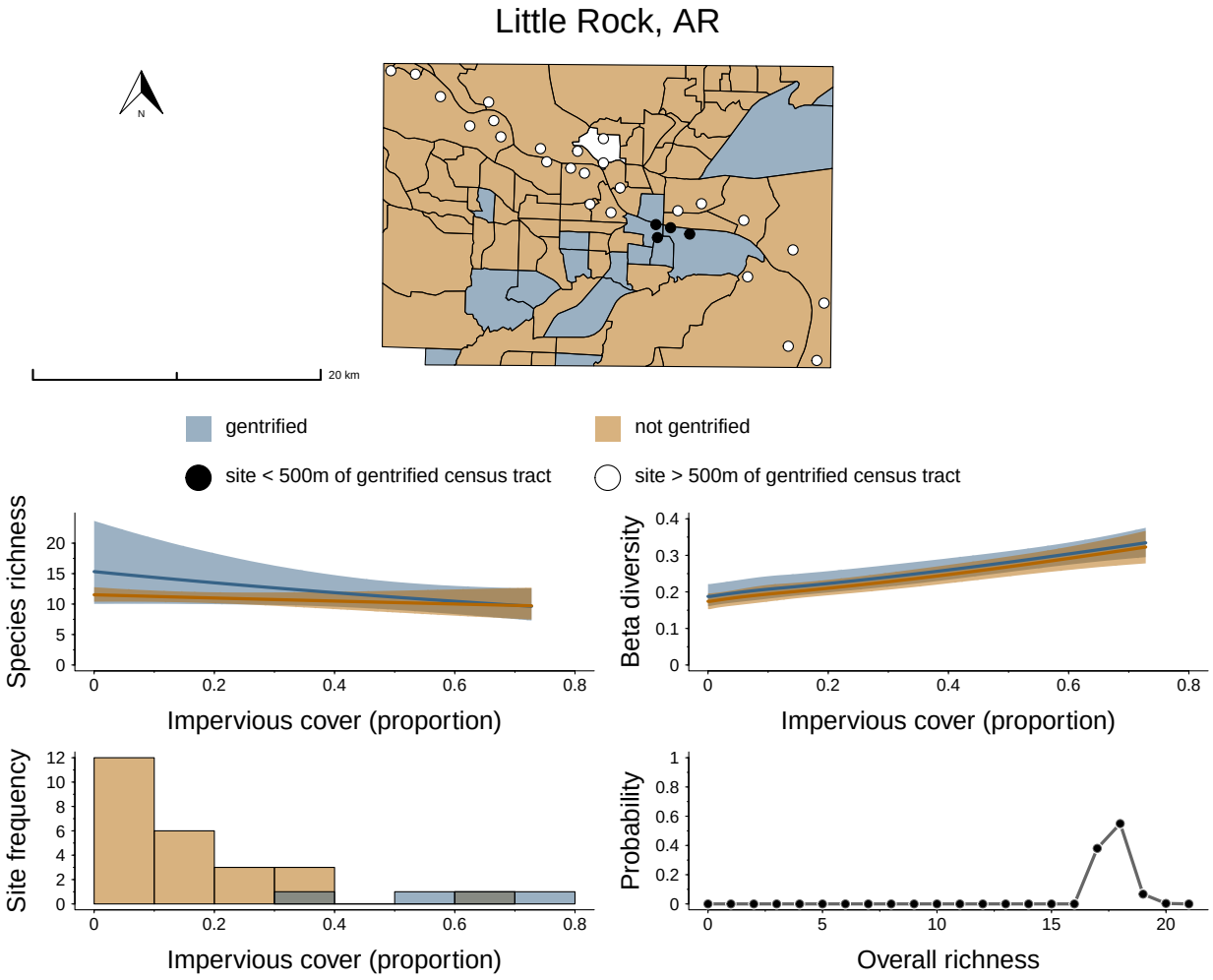

Figure S11. The distribution of gentrifying and non-gentrifying census tracts for Little Rock, AR as well as the camera trap locations for this city. Below the map are city specific estimates for how alpha diversity (species richness) and beta diversity (Bray-Curtis distance) varies at gentrifying and non-gentrifying sites along a gradient of impervious cover. The lower left histogram shows the proportion of impervious cover at gentrifying and non-gentrifying camera trap locations for Little Rock, AR. Finally, the lower right plot shows the estimate for total species richness of medium to large mammals for the city (i.e., gamma diversity).

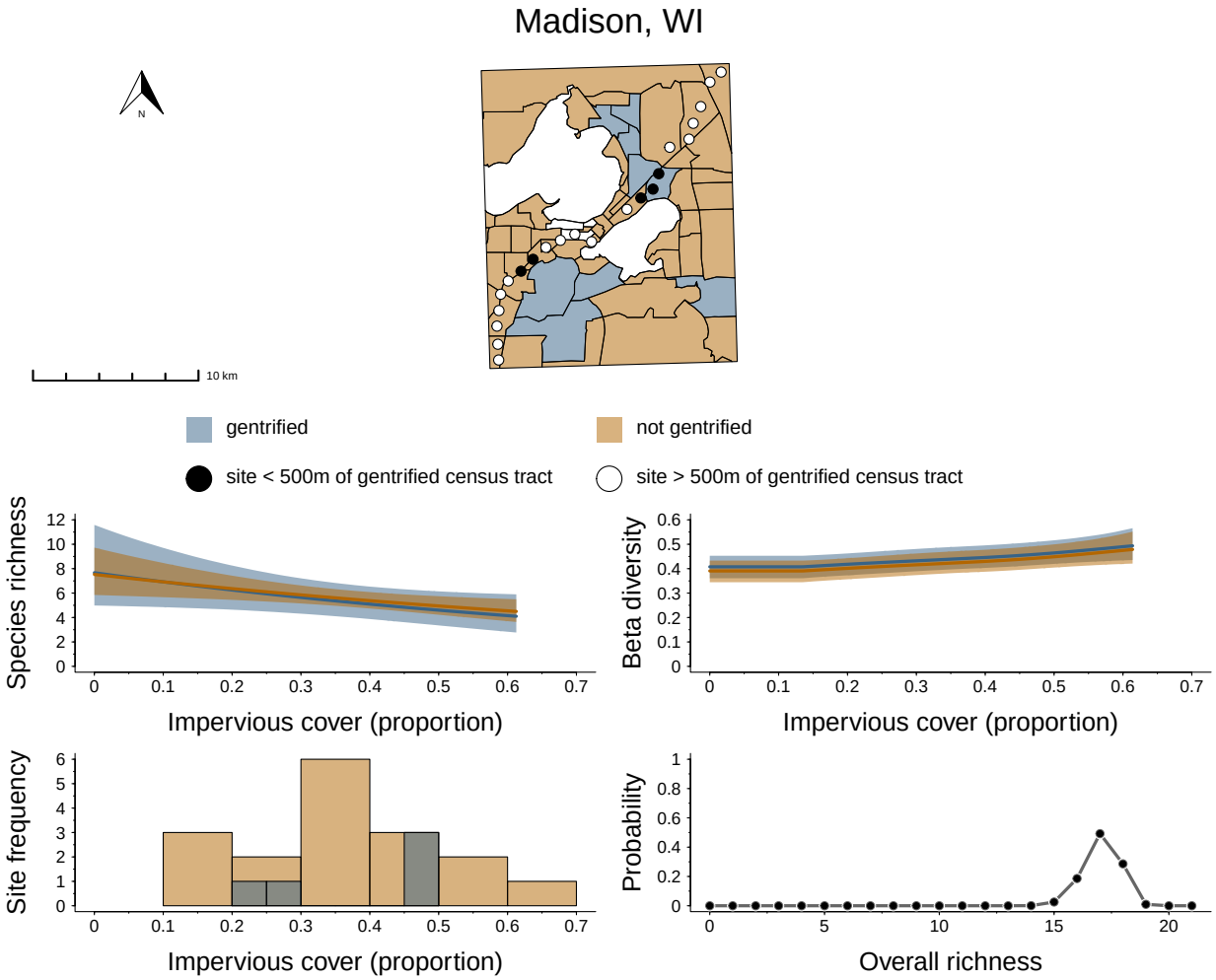

Figure S12. The distribution of gentrifying and non-gentrifying census tracts for Madison, WI as well as the camera trap locations for this city. Below the map are city specific estimates for how alpha diversity (species richness) and beta diversity (Bray-Curtis distance) varies at gentrifying and non-gentrifying sites along a gradient of impervious cover. The lower left histogram shows the proportion of impervious cover at gentrifying and non-gentrifying camera trap locations for Madison, WI. Finally, the lower right plot shows the estimate for total species richness of medium to large mammals for the city (i.e., gamma diversity).

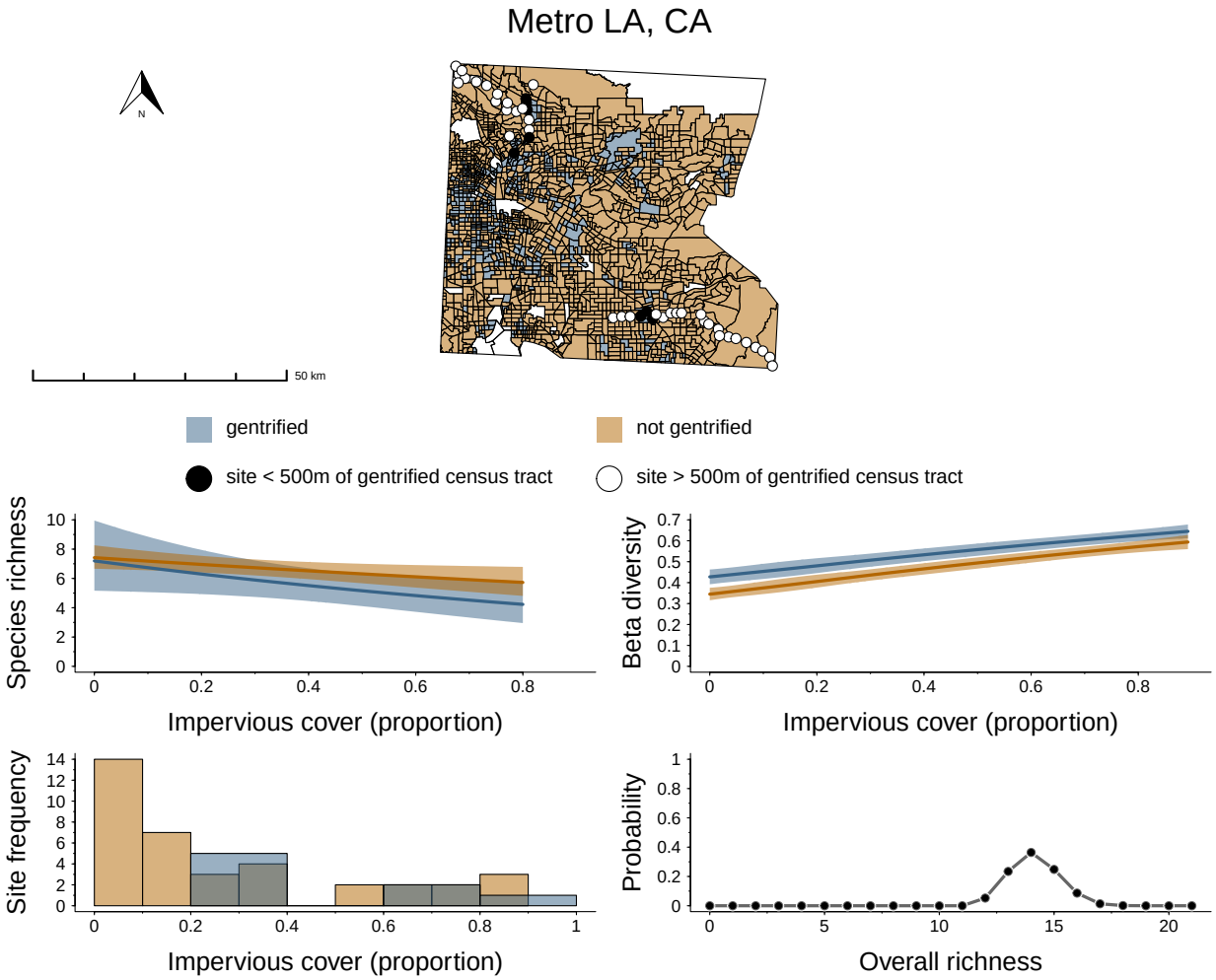

Figure S13. The distribution of gentrifying and non-gentrifying census tracts for Metro LA, CA as well as the camera trap locations for this city. Below the map are city specific estimates for how alpha diversity (species richness) and beta diversity (Bray-Curtis distance) varies at gentrifying and non-gentrifying sites along a gradient of impervious cover. The lower left histogram shows the proportion of impervious cover at gentrifying and non-gentrifying camera trap locations for Metro LA, CA. Finally, the lower right plot shows the estimate for total species richness of medium to large mammals for the city (i.e., gamma diversity).

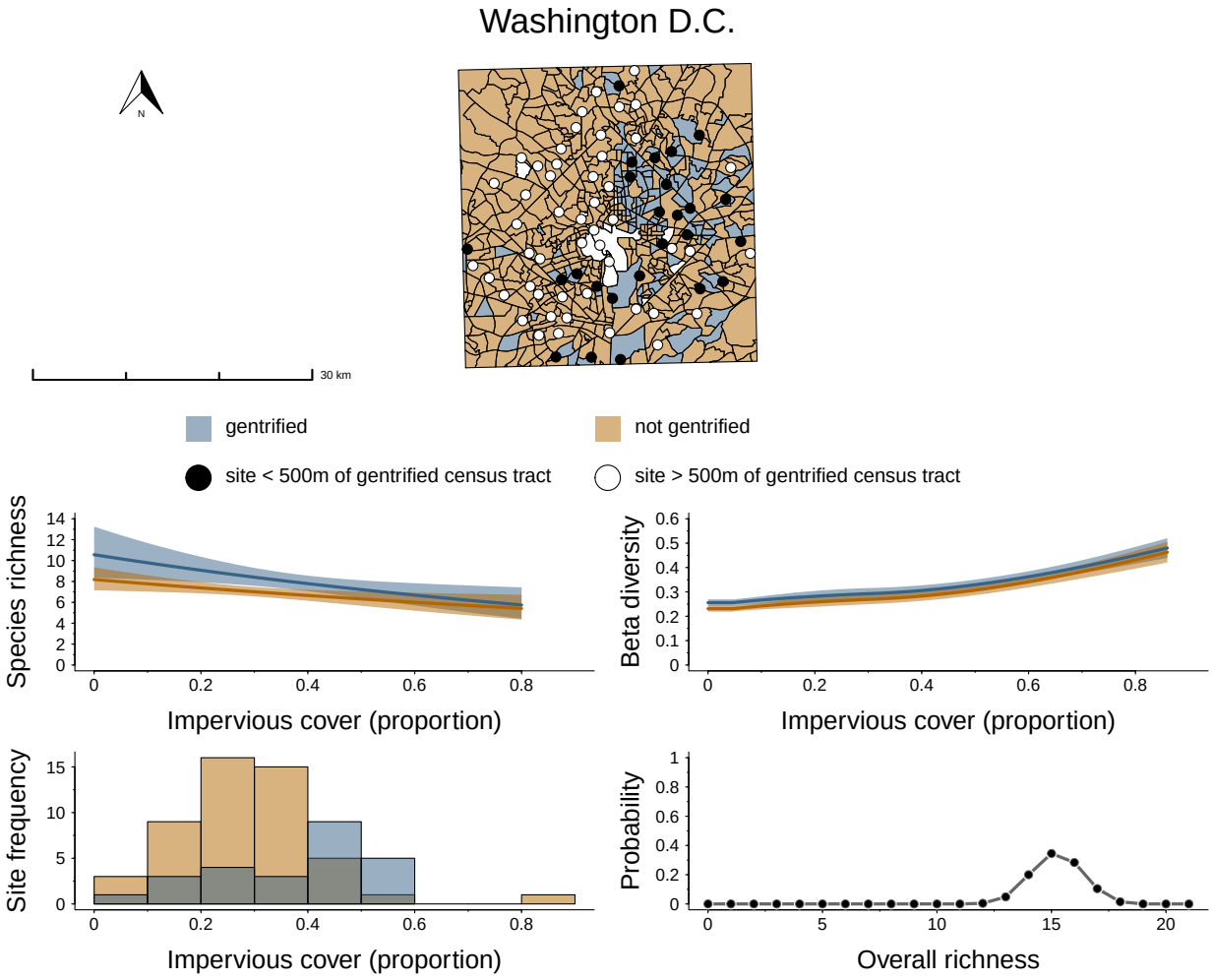

Figure S14. The distribution of gentrifying and non-gentrifying census tracts for Washington D.C. as well as the camera trap locations for this city. Below the map are city specific estimates for how alpha diversity (species richness) and beta diversity (Bray-Curtis distance) varies at gentrifying and non-gentrifying sites along a gradient of impervious cover. The lower left histogram shows the proportion of impervious cover at gentrifying and non-gentrifying camera trap locations for Washington D.C.. Finally, the lower right plot shows the estimate for total species richness of medium to large mammals for the city (i.e., gamma diversity).

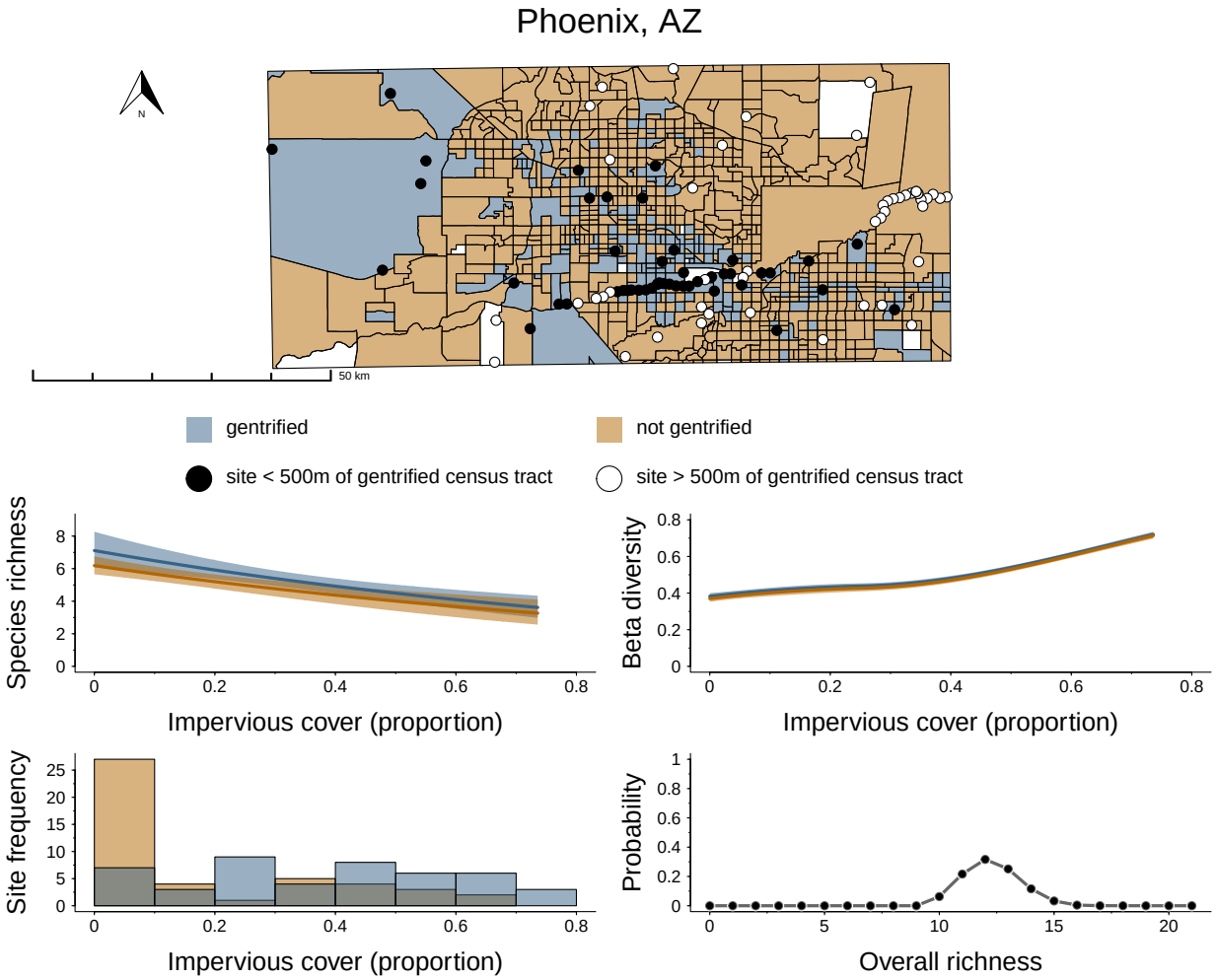

Figure S15. The distribution of gentrifying and non-gentrifying census tracts for Phoenix, AZ as well as the camera trap locations for this city. Below the map are city specific estimates for how alpha diversity (species richness) and beta diversity (Bray-Curtis distance) varies at gentrifying and non-gentrifying sites along a gradient of impervious cover. The lower left histogram shows the proportion of impervious cover at gentrifying and non-gentrifying camera trap locations for Phoenix, AZ. Finally, the lower right plot shows the estimate for total species richness of medium to large mammals for the city (i.e., gamma diversity).

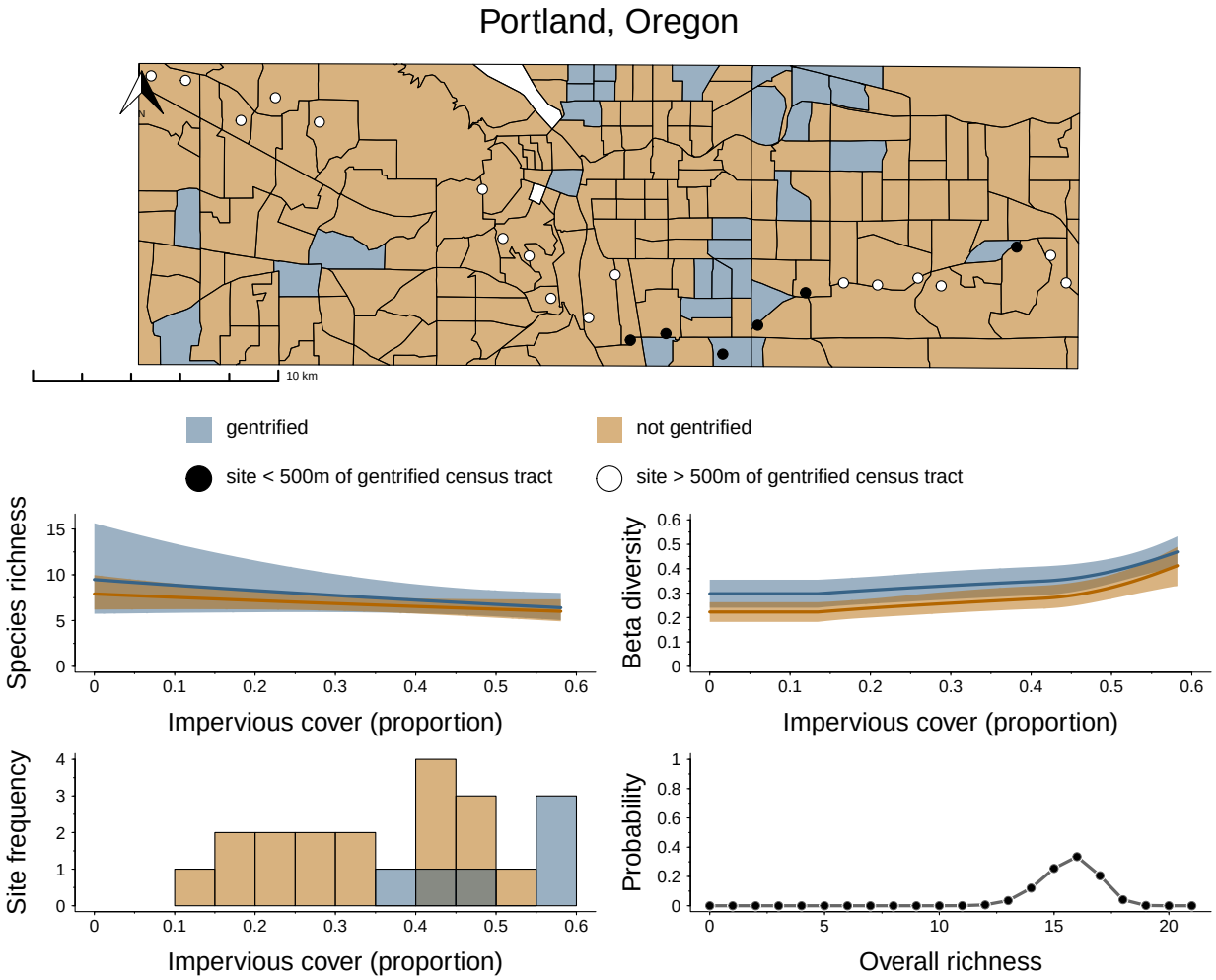

Figure S16. The distribution of gentrifying and non-gentrifying census tracts for Portland, Oregon as well as the camera trap locations for this city. Below the map are city specific estimates for how alpha diversity (species richness) and beta diversity (Bray-Curtis distance) varies at gentrifying and non-gentrifying sites along a gradient of impervious cover. The lower left histogram shows the proportion of impervious cover at gentrifying and non-gentrifying camera trap locations for Portland, Oregon. Finally, the lower right plot shows the estimate for total species richness of medium to large mammals for the city (i.e., gamma diversity).

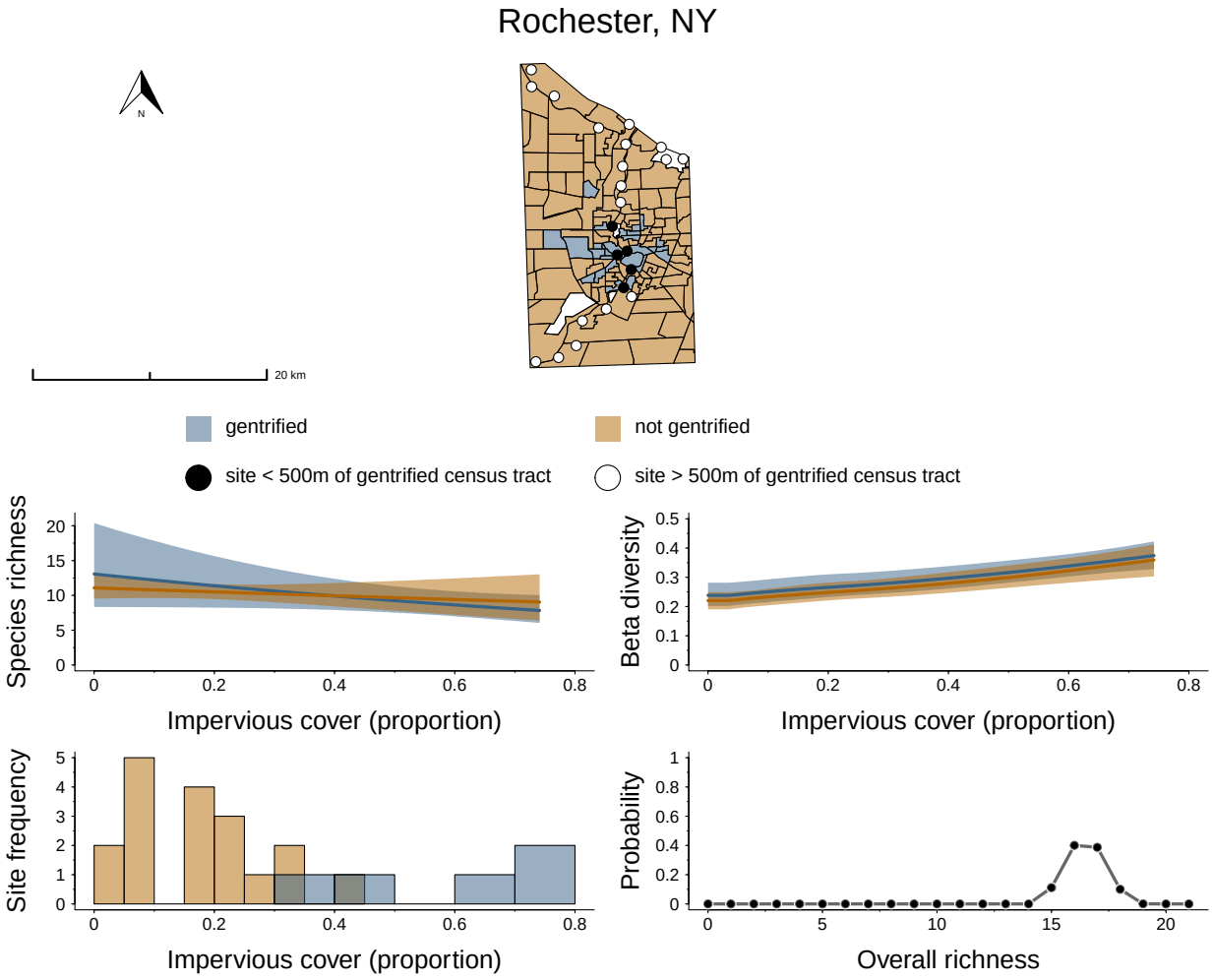

Figure S17. The distribution of gentrifying and non-gentrifying census tracts for Rochester, NY as well as the camera trap locations for this city. Below the map are city specific estimates for how alpha diversity (species richness) and beta diversity (Bray-Curtis distance) varies at gentrifying and non-gentrifying sites along a gradient of impervious cover. The lower left histogram shows the proportion of impervious cover at gentrifying and non-gentrifying camera trap locations for Rochester, NY. Finally, the lower right plot shows the estimate for total species richness of medium to large mammals for the city (i.e., gamma diversity).

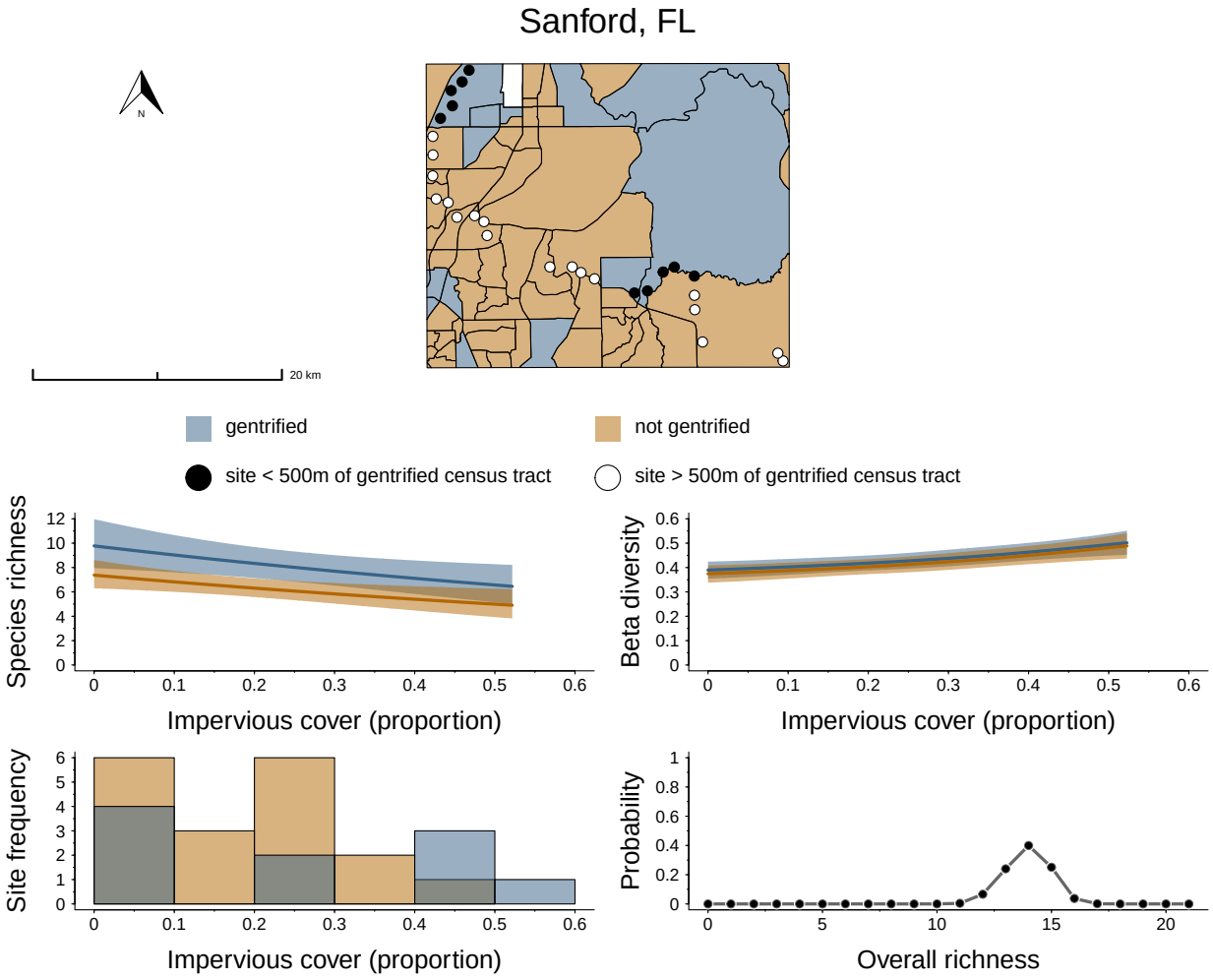

Figure S18. The distribution of gentrifying and non-gentrifying census tracts for Sanford, FL as well as the camera trap locations for this city. Below the map are city specific estimates for how alpha diversity (species richness) and beta diversity (Bray-Curtis distance) varies at gentrifying and non-gentrifying sites along a gradient of impervious cover. The lower left histogram shows the proportion of impervious cover at gentrifying and non-gentrifying camera trap locations for Sanford, FL. Finally, the lower right plot shows the estimate for total species richness of medium to large mammals for the city (i.e., gamma diversity).

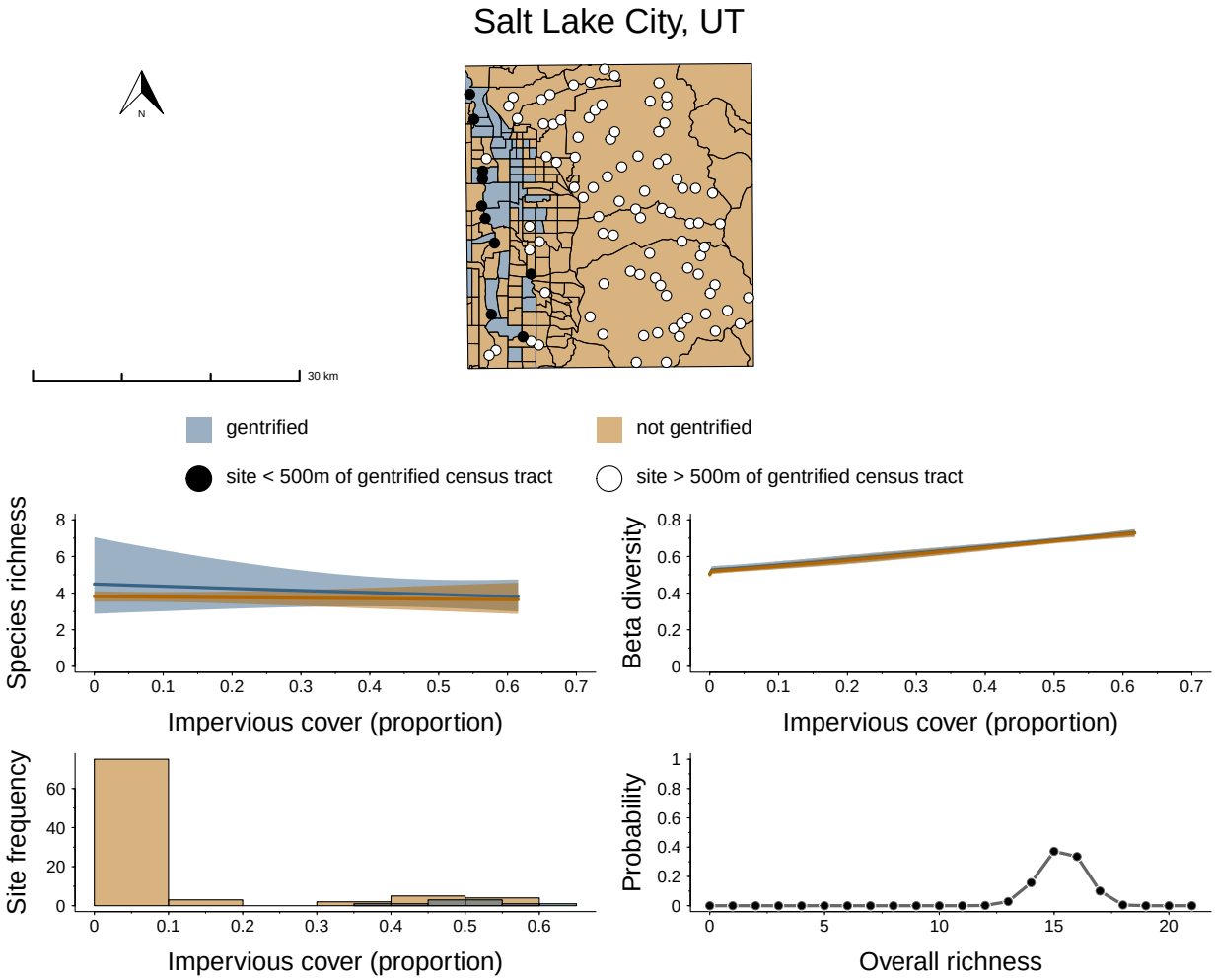

Figure S19. The distribution of gentrifying and non-gentrifying census tracts for Salt Lake City, UT as well as the camera trap locations for this city. Below the map are city specific estimates for how alpha diversity (species richness) and beta diversity (Bray-Curtis distance) varies at gentrifying and non-gentrifying sites along a gradient of impervious cover. The lower left histogram shows the proportion of impervious cover at gentrifying and non-gentrifying camera trap locations for Salt Lake City, UT. Finally, the lower right plot shows the estimate for total species richness of medium to large mammals for the city (i.e., gamma diversity).

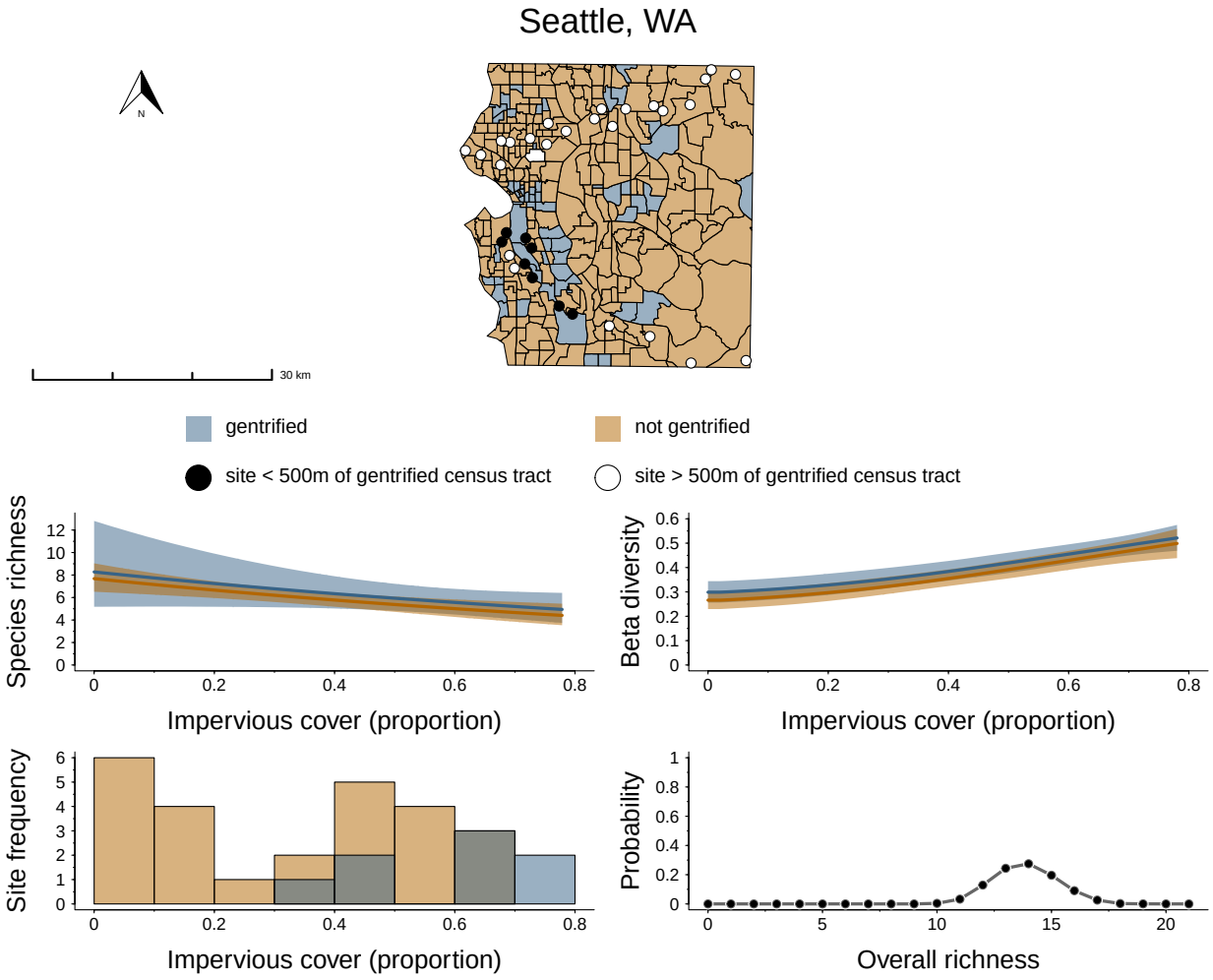

Figure S20. The distribution of gentrifying and non-gentrifying census tracts for Seattle, WA as well as the camera trap locations for this city. Below the map are city specific estimates for how alpha diversity (species richness) and beta diversity (Bray-Curtis distance) varies at gentrifying and non-gentrifying sites along a gradient of impervious cover. The lower left histogram shows the proportion of impervious cover at gentrifying and non-gentrifying camera trap locations for Seattle, WA. Finally, the lower right plot shows the estimate for total species richness of medium to large mammals for the city (i.e., gamma diversity).

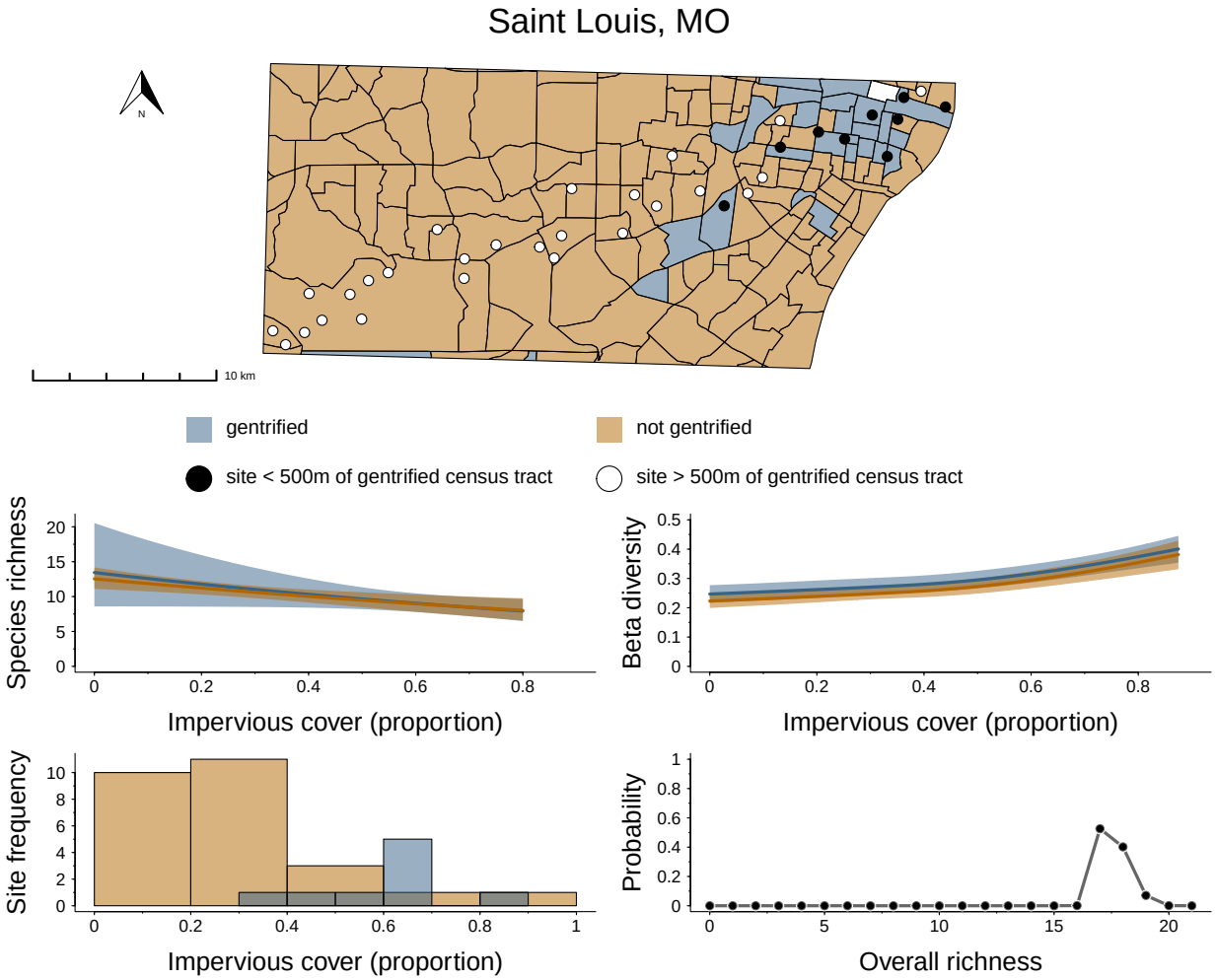

Figure S21. The distribution of gentrifying and non-gentrifying census tracts for Saint Louis, MO as well as the camera trap locations for this city. Below the map are city specific estimates for how alpha diversity (species richness) and beta diversity (Bray-Curtis distance) varies at gentrifying and non-gentrifying sites along a gradient of impervious cover. The lower left histogram shows the proportion of impervious cover at gentrifying and non-gentrifying camera trap locations for Saint Louis, MO. Finally, the lower right plot shows the estimate for total species richness of medium to large mammals for the city (i.e., gamma diversity).

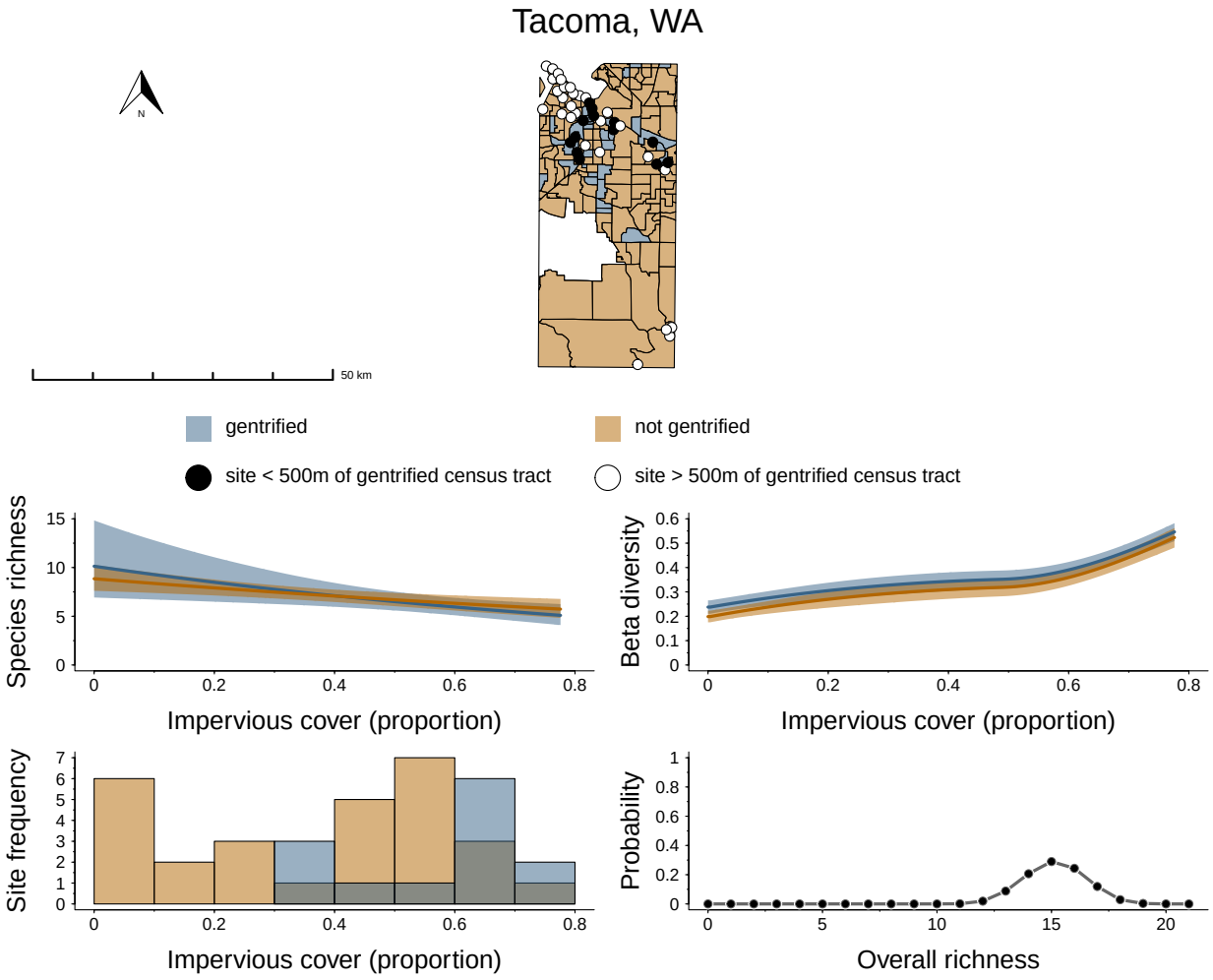

Figure S22. The distribution of gentrifying and non-gentrifying census tracts for Tacoma, WA as well as the camera trap locations for this city. Below the map are city specific estimates for how alpha diversity (species richness) and beta diversity (Bray-Curtis distance) varies at gentrifying and non-gentrifying sites along a gradient of impervious cover. The lower left histogram shows the proportion of impervious cover at gentrifying and non-gentrifying camera trap locations for Tacoma, WA. Finally, the lower right plot shows the estimate for total species richness of medium to large mammals for the city (i.e., gamma diversity).

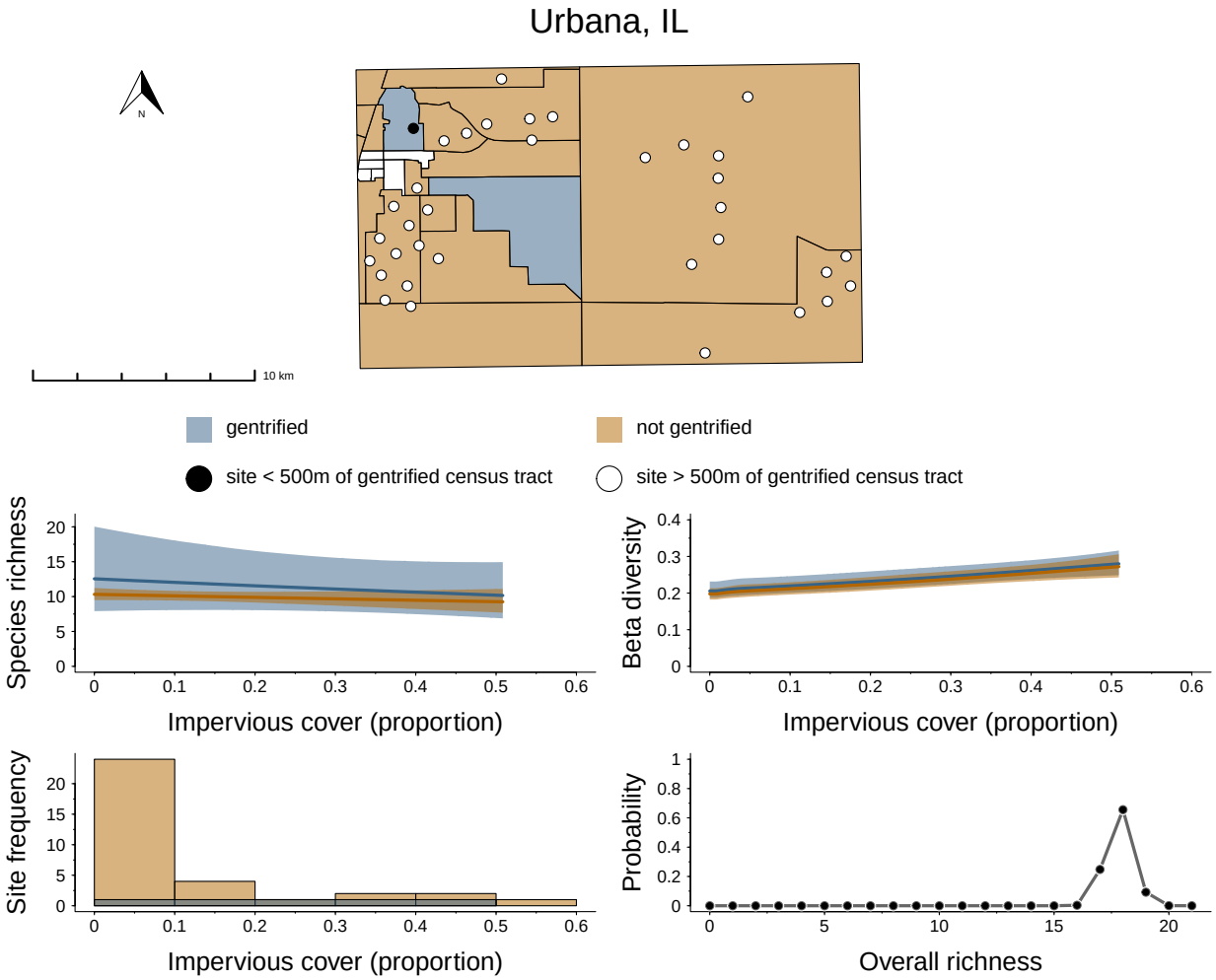

Figure S23. The distribution of gentrifying and non-gentrifying census tracts for Urbana, IL as well as the camera trap locations for this city. Below the map are city specific estimates for how alpha diversity (species richness) and beta diversity (Bray-Curtis distance) varies at gentrifying and non-gentrifying sites along a gradient of impervious cover. The lower left histogram shows the proportion of impervious cover at gentrifying and non-gentrifying camera trap locations for Urbana, IL. Finally, the lower right plot shows the estimate for total species richness of medium to large mammals for the city (i.e., gamma diversity).

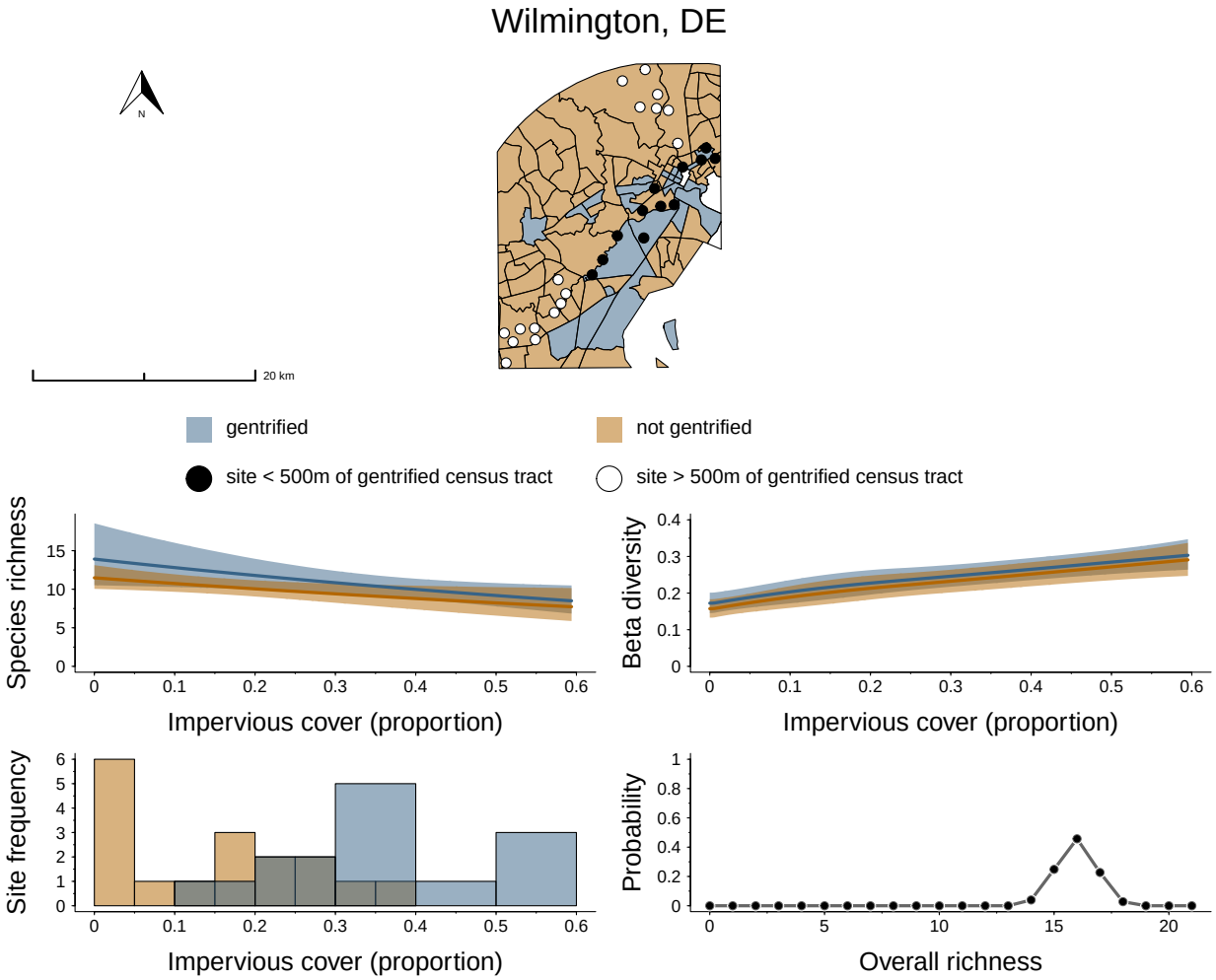

Figure S24. The distribution of gentrifying and non-gentrifying census tracts for Wilmington, DE as well as the camera trap locations for this city. Below the map are city specific estimates for how alpha diversity (species richness) and beta diversity (Bray-Curtis distance) varies at gentrifying and non-gentrifying sites along a gradient of impervious cover. The lower left histogram shows the proportion of impervious cover at gentrifying and non-gentrifying camera trap locations for Wilmington, DE. Finally, the lower right plot shows the estimate for total species richness of medium to large mammals for the city (i.e., gamma diversity).

Alpha diversity model estimates

Table S10: The among-city average estimates from the alpha diversity model.

Parameter	CI(0.025)	CI(0.05)	Estimate	CI(0.95)	CI(0.975)
intercept	1.98	2.01	2.16	2.30	2.33
gent	-0.01	0.02	0.17	0.33	0.36
imp	-0.71	-0.67	-0.49	-0.31	-0.27
gent X imp	-0.53	-0.48	-0.22	0.04	0.09

Table S11: The estimated standard deviation of city-specific estimates from the among-city means from the alpha diversity model.

Parameter	CI(0.025)	CI(0.05)	Estimate	CI(0.95)	CI(0.975)
intercept	0.31	0.32	0.40	0.53	0.56
gent	0.27	0.28	0.35	0.46	0.49
imp	0.32	0.34	0.44	0.59	0.63
gent X imp	0.33	0.35	0.47	0.65	0.70

Table S12: City specific-estimates from the alpha diversity model.

City	Parameter	CI(0.025)	CI(0.05)	Estimate	CI(0.95)	CI(0.975)
Athens, GA	intercept	2.02	2.05	2.16	2.28	2.30
	gent	-0.09	-0.04	0.24	0.51	0.57
	imp	-1.29	-1.21	-0.78	-0.35	-0.27
	gent X imp	-0.83	-0.69	0.02	0.79	0.96
Bay Area, CA	intercept	1.85	1.88	2.01	2.14	2.17
	gent	-0.29	-0.21	0.15	0.52	0.59
	imp	-1.01	-0.95	-0.68	-0.40	-0.35
	gent X imp	-1.01	-0.89	-0.29	0.30	0.42
Boston, MA	intercept	2.02	2.05	2.20	2.35	2.38
	gent	-0.10	-0.03	0.28	0.60	0.66
	imp	-0.82	-0.75	-0.34	0.08	0.16
	gent X imp	-0.99	-0.88	-0.28	0.31	0.43
Chicago, IL	intercept	2.32	2.34	2.43	2.53	2.55
	gent	0.11	0.15	0.34	0.54	0.59
	imp	-0.94	-0.90	-0.69	-0.48	-0.44
	gent X imp	-0.94	-0.87	-0.51	-0.17	-0.09
Denver, CO	intercept	1.73	1.77	1.94	2.12	2.15
	gent	-0.07	-0.02	0.27	0.56	0.61
	imp	-0.83	-0.75	-0.35	0.06	0.14
	gent X imp	-0.95	-0.83	-0.25	0.34	0.46
Houston, TX	intercept	2.18	2.21	2.38	2.55	2.58
	gent	-0.25	-0.18	0.15	0.47	0.53
	imp	-1.31	-1.24	-0.87	-0.50	-0.43
	gent X imp	-0.88	-0.77	-0.21	0.34	0.45
Indianapolis, IN	intercept	2.22	2.25	2.37	2.49	2.51
	gent	-0.19	-0.15	0.10	0.34	0.39
	imp	-0.52	-0.46	-0.11	0.23	0.30
	gent X imp	-0.75	-0.65	-0.14	0.37	0.48
Iowa City, IA	intercept	2.43	2.44	2.53	2.61	2.63
	gent	-0.20	-0.15	0.08	0.31	0.36
	imp	-0.87	-0.80	-0.46	-0.11	-0.05
	gent X imp	-0.90	-0.78	-0.16	0.46	0.59
Jackson, MS	intercept	1.83	1.85	1.97	2.09	2.12
	gent	0.01	0.06	0.31	0.57	0.63
	imp	-0.69	-0.62	-0.24	0.14	0.21
	gent X imp	-1.36	-1.23	-0.61	-0.02	0.08
Little Rock, AR	intercept	2.34	2.36	2.45	2.53	2.55

	gent	-0.13	-0.07	0.28	0.62	0.69
	imp	-0.66	-0.59	-0.24	0.13	0.20
	gent X imp	-1.12	-1.00	-0.39	0.22	0.33
Madison, WI	intercept	1.76	1.80	2.02	2.23	2.27
	gent	-0.38	-0.31	0.01	0.33	0.39
	imp	-1.49	-1.38	-0.83	-0.32	-0.21
	gent X imp	-1.02	-0.88	-0.18	0.54	0.68
Metro LA, CA	intercept	1.90	1.91	2.00	2.09	2.11
	gent	-0.36	-0.31	-0.03	0.24	0.29
	imp	-0.60	-0.56	-0.32	-0.09	-0.05
	gent X imp	-1.01	-0.89	-0.34	0.20	0.30
Washington D.C.	intercept	1.97	1.99	2.10	2.21	2.23
	gent	0.02	0.06	0.26	0.46	0.50
	imp	-0.93	-0.86	-0.52	-0.18	-0.11
	gent X imp	-0.87	-0.77	-0.26	0.25	0.35
Phoenix, AZ	intercept	1.73	1.75	1.82	1.90	1.91
	gent	-0.03	-0.01	0.14	0.28	0.31
	imp	-1.23	-1.18	-0.87	-0.58	-0.52
	gent X imp	-0.53	-0.45	-0.05	0.36	0.45
Portland, Oregon	intercept	1.83	1.87	2.07	2.27	2.30
	gent	-0.26	-0.18	0.18	0.54	0.61
	imp	-1.11	-1.01	-0.48	0.06	0.16
	gent X imp	-1.02	-0.88	-0.20	0.48	0.62
Rochester, NY	intercept	2.26	2.28	2.41	2.53	2.55
	gent	-0.26	-0.19	0.16	0.52	0.58
	imp	-0.87	-0.78	-0.28	0.24	0.34
	gent X imp	-1.16	-1.03	-0.41	0.19	0.31
Sanford, FL	intercept	1.84	1.86	2.00	2.13	2.15
	gent	0.05	0.09	0.28	0.48	0.52
	imp	-1.40	-1.30	-0.78	-0.29	-0.19
	gent X imp	-0.71	-0.60	-0.02	0.59	0.71
Salt Lake City, UT	intercept	1.26	1.27	1.34	1.40	1.41
	gent	-0.27	-0.20	0.17	0.52	0.59
	imp	-0.49	-0.42	-0.07	0.26	0.32
	gent X imp	-1.00	-0.87	-0.20	0.48	0.62
Seattle, WA	intercept	1.87	1.90	2.04	2.17	2.20
	gent	-0.37	-0.29	0.08	0.43	0.49
	imp	-1.13	-1.06	-0.71	-0.37	-0.30
	gent X imp	-0.65	-0.54	0.04	0.66	0.80
Saint Louis, MO	intercept	2.40	2.42	2.53	2.63	2.65
	gent	-0.37	-0.30	0.06	0.42	0.49
	imp	-0.90	-0.84	-0.56	-0.26	-0.21
	gent X imp	-0.77	-0.66	-0.09	0.48	0.60
Tacoma, WA	intercept	2.03	2.05	2.18	2.30	2.32
	gent	-0.24	-0.18	0.13	0.44	0.50
	imp	-0.89	-0.84	-0.55	-0.27	-0.22
	gent X imp	-0.96	-0.86	-0.33	0.20	0.31
Urbana, IL	intercept	2.25	2.26	2.33	2.40	2.42
	gent	-0.26	-0.19	0.20	0.57	0.65
	imp	-0.65	-0.58	-0.22	0.15	0.21

	gent X imp	-1.11	-0.95	-0.20	0.55	0.72
Wilmington, DE	intercept	2.31	2.33	2.44	2.55	2.57
	gent	-0.08	-0.04	0.19	0.42	0.47
	imp	-1.25	-1.16	-0.68	-0.21	-0.12
	gent X imp	-0.87	-0.75	-0.16	0.44	0.56

Beta diversity model estimates

Table S13: The among-city average estimates from the beta diversity model. Note that the two continous covariates (geographic distance and impervious cover) have been transformed with I-splines, so each covariate has multiple slope terms.

Parameter	Spline	CI(0.025)	CI(0.05)	Estimate	CI(0.95)	CI(0.975)
intercept		0	0.01	0.06	0.20	0.23
distance	1	0	0.00	0.01	0.06	0.07
	2	0	0.00	0.01	0.05	0.07
	3	0	0.00	0.01	0.06	0.07
imp	1	0	0.00	0.01	0.06	0.07
	2	0	0.00	0.02	0.07	0.08
	3	0	0.00	0.03	0.11	0.13
gent		0	0.00	0.01	0.05	0.07

Table S14: The estimated standard deviation of city-specific estimates from the among-city means from the beta diversity model. Note that the two continous covariates (geographic distance and impervious cover) have been transformed with I-splines, so each covariate has multiple slope terms.

Parameter	Spline	CI(0.025)	CI(0.05)	Estimate	CI(0.95)	CI(0.975)
intercept		0.29	0.31	0.39	0.51	0.54
distance	1	0.23	0.24	0.30	0.39	0.41
	2	0.23	0.24	0.30	0.39	0.41
	3	0.23	0.24	0.30	0.39	0.41
imp	1	0.24	0.25	0.31	0.40	0.42
	2	0.24	0.25	0.31	0.40	0.42
	3	0.28	0.29	0.36	0.47	0.49
gent		0.23	0.24	0.30	0.38	0.41

Table S15: City specific-estimates from the beta diversity model. Note that the two continous covariates (geographic distance and impervious cover) have been transformed with I-splines, so each covariate has multiple slope terms.

City	Spline	Parameter	CI(0.025)	CI(0.05)	Estimate	CI(0.95)	CI(0.975)
Athens, GA	intercept		0.24	0.25	0.29	0.32	0.33
	distance	1	0.00	0.00	0.02	0.07	0.08
		2	0.00	0.00	0.01	0.05	0.06
		3	0.00	0.00	0.02	0.09	0.10
	imp	1	0.00	0.00	0.01	0.04	0.05
		2	0.00	0.00	0.02	0.07	0.08
		3	0.07	0.09	0.17	0.26	0.27

	gent		0.00	0.00	0.01	0.03	0.04
Bay Area, CA	intercept		0.13	0.14	0.20	0.26	0.27
	distance	1	0.07	0.08	0.18	0.27	0.29
		2	0.16	0.17	0.25	0.32	0.34
		3	0.00	0.00	0.03	0.10	0.12
	imp	1	0.15	0.17	0.24	0.31	0.33
		2	0.00	0.00	0.03	0.09	0.11
		3	0.12	0.14	0.21	0.29	0.31
	gent		0.01	0.01	0.06	0.10	0.11
Boston, MA	intercept		0.20	0.21	0.26	0.30	0.30
	distance	1	0.00	0.00	0.03	0.09	0.10
		2	0.00	0.00	0.02	0.07	0.08
		3	0.00	0.00	0.05	0.14	0.17
	imp	1	0.00	0.00	0.04	0.10	0.12
		2	0.00	0.00	0.03	0.10	0.11
		3	0.01	0.01	0.07	0.15	0.17
	gent		0.00	0.00	0.01	0.05	0.05
Chicago, IL	intercept		0.23	0.24	0.25	0.26	0.27
	distance	1	0.00	0.00	0.01	0.02	0.03
		2	0.00	0.00	0.01	0.02	0.03
		3	0.01	0.02	0.06	0.10	0.11
	imp	1	0.00	0.00	0.01	0.02	0.03
		2	0.07	0.07	0.10	0.13	0.13
		3	0.21	0.21	0.24	0.26	0.27
	gent		0.00	0.00	0.01	0.02	0.03
Denver, CO	intercept		0.26	0.27	0.32	0.36	0.36
	distance	1	0.00	0.00	0.03	0.09	0.11
		2	0.00	0.00	0.02	0.07	0.08
		3	0.00	0.00	0.04	0.13	0.16
	imp	1	0.22	0.23	0.33	0.41	0.43
		2	0.00	0.00	0.05	0.14	0.15
		3	0.00	0.00	0.02	0.07	0.09
	gent		0.00	0.00	0.03	0.07	0.07
Houston, TX	intercept		0.17	0.18	0.22	0.26	0.27
	distance	1	0.00	0.00	0.01	0.05	0.06
		2	0.00	0.00	0.01	0.03	0.04
		3	0.00	0.00	0.02	0.07	0.08
	imp	1	0.00	0.00	0.01	0.03	0.04
		2	0.07	0.09	0.17	0.25	0.26
		3	0.01	0.02	0.09	0.16	0.18
	gent		0.00	0.00	0.03	0.08	0.09
Indianapolis, IN	intercept		0.17	0.17	0.20	0.23	0.23
	distance	1	0.00	0.00	0.02	0.06	0.07
		2	0.00	0.00	0.01	0.04	0.04
		3	0.00	0.00	0.04	0.10	0.12
	imp	1	0.00	0.00	0.01	0.03	0.04
		2	0.00	0.00	0.03	0.07	0.08
		3	0.00	0.00	0.02	0.05	0.06
	gent		0.00	0.00	0.02	0.04	0.04
Iowa City, IA	intercept		0.08	0.09	0.11	0.14	0.14

	distance	1	0.00	0.00	0.02	0.06	0.06
		2	0.00	0.00	0.01	0.04	0.04
		3	0.00	0.00	0.02	0.07	0.08
	imp	1	0.00	0.00	0.01	0.04	0.04
		2	0.00	0.00	0.02	0.06	0.07
		3	0.03	0.04	0.09	0.13	0.14
	gent		0.00	0.00	0.02	0.04	0.04
Jackson, MS	intercept		0.36	0.37	0.41	0.46	0.46
	distance	1	0.00	0.00	0.03	0.09	0.11
		2	0.00	0.01	0.06	0.13	0.14
		3	0.00	0.01	0.08	0.23	0.26
	imp	1	0.00	0.00	0.01	0.02	0.03
		2	0.00	0.01	0.05	0.12	0.13
		3	0.01	0.01	0.07	0.15	0.17
	gent		0.03	0.04	0.07	0.11	0.12
Little Rock, AR	intercept		0.14	0.14	0.17	0.19	0.20
	distance	1	0.00	0.00	0.02	0.05	0.06
		2	0.00	0.00	0.01	0.04	0.04
		3	0.00	0.00	0.03	0.10	0.11
	imp	1	0.00	0.00	0.02	0.05	0.05
		2	0.01	0.01	0.07	0.13	0.14
		3	0.03	0.04	0.11	0.19	0.20
	gent		0.00	0.00	0.01	0.05	0.05
Madison, WI	intercept		0.30	0.31	0.39	0.47	0.48
	distance	1	0.00	0.01	0.07	0.18	0.20
		2	0.00	0.01	0.08	0.19	0.22
		3	0.00	0.01	0.07	0.22	0.26
	imp	1	0.00	0.00	0.03	0.10	0.12
		2	0.00	0.00	0.05	0.15	0.17
		3	0.00	0.00	0.06	0.18	0.21
	gent		0.00	0.00	0.02	0.08	0.09
Metro LA, CA	intercept		0.33	0.34	0.38	0.41	0.42
	distance	1	0.00	0.00	0.03	0.09	0.10
		2	0.00	0.00	0.01	0.05	0.06
		3	0.00	0.00	0.02	0.09	0.10
	imp	1	0.00	0.01	0.05	0.11	0.12
		2	0.11	0.13	0.24	0.34	0.35
		3	0.06	0.08	0.19	0.30	0.32
	gent		0.08	0.09	0.13	0.18	0.19
Washington D.C.	intercept		0.18	0.18	0.21	0.24	0.25
	distance	1	0.01	0.01	0.04	0.08	0.08
		2	0.00	0.00	0.01	0.03	0.04
		3	0.00	0.00	0.01	0.05	0.06
	imp	1	0.00	0.01	0.04	0.07	0.07
		2	0.00	0.01	0.05	0.09	0.10
		3	0.19	0.20	0.28	0.35	0.36
	gent		0.02	0.02	0.03	0.05	0.05
Phoenix, AZ	intercept		0.28	0.29	0.32	0.36	0.36
	distance	1	0.08	0.09	0.13	0.18	0.19
		2	0.00	0.00	0.02	0.06	0.07

		3	0.00	0.00	0.03	0.09	0.11
	imp	1	0.03	0.04	0.08	0.11	0.12
		2	0.00	0.01	0.05	0.11	0.12
		3	0.58	0.60	0.66	0.72	0.74
	gent		0.00	0.00	0.02	0.04	0.04
Portland, Oregon	intercept		0.15	0.16	0.21	0.26	0.27
	distance	1	0.00	0.00	0.03	0.08	0.10
		2	0.00	0.00	0.02	0.06	0.07
		3	0.00	0.00	0.04	0.13	0.15
	imp	1	0.00	0.00	0.04	0.11	0.13
		2	0.00	0.00	0.04	0.12	0.14
		3	0.06	0.08	0.18	0.30	0.32
	gent		0.03	0.04	0.10	0.17	0.18
Rochester, NY	intercept		0.17	0.18	0.22	0.25	0.26
	distance	1	0.00	0.00	0.02	0.07	0.08
		2	0.00	0.00	0.01	0.05	0.06
		3	0.00	0.00	0.03	0.09	0.10
	imp	1	0.00	0.00	0.02	0.07	0.08
		2	0.00	0.01	0.05	0.14	0.16
		3	0.02	0.03	0.11	0.19	0.20
	gent		0.00	0.00	0.02	0.06	0.07
Sanford, FL	intercept		0.33	0.35	0.41	0.46	0.47
	distance	1	0.00	0.00	0.04	0.13	0.14
		2	0.00	0.00	0.02	0.08	0.09
		3	0.00	0.00	0.05	0.15	0.18
	imp	1	0.00	0.00	0.01	0.06	0.07
		2	0.00	0.01	0.07	0.18	0.20
		3	0.01	0.02	0.10	0.21	0.23
	gent		0.00	0.00	0.02	0.06	0.07
Salt Lake City, UT	intercept		0.57	0.58	0.64	0.68	0.69
	distance	1	0.00	0.01	0.05	0.12	0.13
		2	0.00	0.00	0.02	0.06	0.07
		3	0.00	0.01	0.06	0.18	0.21
	imp	1	0.00	0.01	0.04	0.08	0.08
		2	0.05	0.06	0.17	0.28	0.30
		3	0.23	0.25	0.39	0.53	0.56
	gent		0.00	0.00	0.01	0.04	0.04
Seattle, WA	intercept		0.15	0.16	0.22	0.27	0.27
	distance	1	0.00	0.00	0.04	0.12	0.14
		2	0.01	0.02	0.11	0.22	0.24
		3	0.01	0.03	0.19	0.41	0.46
	imp	1	0.00	0.00	0.03	0.09	0.10
		2	0.10	0.12	0.22	0.31	0.33
		3	0.02	0.03	0.13	0.24	0.26
	gent		0.00	0.01	0.04	0.09	0.10
Saint Louis, MO	intercept		0.18	0.19	0.22	0.24	0.25
	distance	1	0.00	0.00	0.02	0.06	0.07
		2	0.00	0.00	0.03	0.09	0.10
		3	0.00	0.01	0.06	0.16	0.18
	imp	1	0.00	0.00	0.01	0.05	0.05

		2	0.00	0.01	0.05	0.12	0.14
		3	0.07	0.09	0.16	0.23	0.24
	gent		0.00	0.01	0.03	0.06	0.07
Tacoma, WA	intercept		0.17	0.17	0.20	0.23	0.23
	distance	1	0.00	0.00	0.01	0.05	0.06
		2	0.00	0.00	0.01	0.05	0.06
		3	0.01	0.01	0.07	0.15	0.17
	imp	1	0.07	0.08	0.14	0.19	0.20
		2	0.00	0.00	0.04	0.10	0.11
		3	0.26	0.28	0.34	0.41	0.42
	gent		0.01	0.02	0.05	0.08	0.09
Urbana, IL	intercept		0.18	0.19	0.21	0.23	0.23
	distance	1	0.00	0.00	0.01	0.03	0.03
		2	0.00	0.00	0.01	0.03	0.04
		3	0.00	0.01	0.05	0.10	0.11
	imp	1	0.00	0.00	0.01	0.02	0.03
		2	0.00	0.00	0.03	0.07	0.08
		3	0.00	0.01	0.06	0.11	0.12
	gent		0.00	0.00	0.01	0.03	0.04
Wilmington, DE	intercept		0.11	0.12	0.14	0.17	0.18
	distance	1	0.00	0.00	0.02	0.05	0.06
		2	0.00	0.00	0.01	0.05	0.06
		3	0.00	0.00	0.04	0.11	0.12
	imp	1	0.01	0.01	0.05	0.10	0.11
		2	0.01	0.01	0.07	0.13	0.14
		3	0.00	0.01	0.05	0.11	0.12
	gent		0.00	0.00	0.02	0.04	0.05